CHARACTERIZATION OF BAF155 AND BAF170
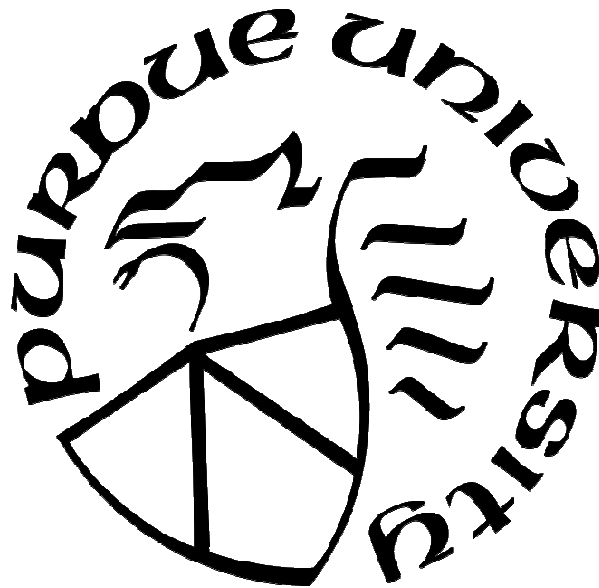# IN EARLY PORCINE EMBRYOGENESIS

by

Hayly Goebel

A Thesis

Submitted to the Faculty of Purdue University

In Partial Fulfillment of the Requirements for the degree of

Master of Science

Department of Animal Sciences

West Lafayette, IN

August 2019

THE PURDUE UNIVERSITY GRADUATE SCHOOL
STATEMENT OF COMMITTEE APPROVAL

Dr. Birgit Cabot

    Department of Animal Science

Dr. Zoltan Machaty

    Department of Animal Science

Dr. Kara Stewart

    Department of Animal Science

Approved by:

    Dr. Ryan Cabot

        Department of Animal Sciences Head of the Graduate Program

Dedicated to Mom and Dad,
who held me up through the not-so-easy times
and reminded me that cowgirls don't cry.

ACKNOWLEDGEMENTS

First I would like to thank my advisor: Dr. Birgit Cabot, without whom none of this would have been possible. To the members of my committee: Dr. Zoltan Machaty and Dr. Kara Stewart, who were there to share their expertise and advise me. To the members of the Cabot laboratory past and present: Dr. Ryan Cabot, Jennifer Crodian, Yu-Chun Tseng, Bethany Weldon, and Jillian Bouck who provided support, answered my questions, and were always there to step in and help when I needed it. Additionally, I would like to thank Natalie Ehmke and Ilka Lorenzo[2] for both their academic and emotional support throughout my graduate years.

Next, I would like to thank my friends and family. Megan Orth and Amy Situ, who are my oldest friends and grew up alongside me. My brothers, Dylan and John whom I love despite ruining the great gig I had going on as an only child. My Momma, who was there for many an anxiety wracked phone call, who most importantly understood, and waited at home for me with open arms. To my Dad, who drove me to push myself above and beyond the necessary and who motivated my love for animal science first by finding my "horsey and barn".

Finally, I would like to thank my partner, Grant Hinkle. He learned early on to ask if I would like "a solution or support" when I vented and he always provided what I needed without question. His constant and unending reinforcement of my goals was and is invaluable to me. I hope that I can give that same support back in the years to come. Thank you and I love you.

TABLE OF CONTENTS

LIST OF TABLES

LIST OF FIGURES

ABSTRACT

The production of developmentally competent *in vitro* derived embryos is necessary to decreasing both economic and emotional losses. Epigenetic abnormalities/insults have been shown to occur at a higher incidence in *in vitro* embryos. An increased prevalence of epigenetic derived disorders such as Parkinson's disease, Prader-Willi syndrome, and α-thalassemia as well as elevated preimplantation embryo arrest and reduced developmental rates are theorized to be caused by errors in the mediation of chromatin remodeling. Chromatin remodeling refers to the restructuring of packaged DNA so that transcription factors are either given more or less access to specific sequences. This can be done by covalent modification through histone methylation, acetylation, and phosphorylation as well as noncovalent modifications which employ ATP dependent chromatin remodeling complexes. The purpose of this thesis was to characterize two structurally integral core subunits, BAF155 and BAF170, of the SWI/SNF chromatin remodeling complex in porcine oocytes and preimplantation embryos.

The first study concentrated on the transcript abundance of *BAF155* and *BAF170* in porcine oocytes and embryos. First, *BAF155* and *BAF170* transcript sequences were identified in porcine muscle and heart tissues. Those sequences were used to create quantitative polymerase chain reaction (qPCR) primers. mRNA from pools of GV oocytes (100-800) was converted to cDNA for transcript abundance measurements. However, transcript abundance remained too low for either *BAF155* or *BAF170* to be accurately quantified.

The second study focused on developmental competency of embryos post interfering RNA (RNAi) knockdown of *BAF155*, *BAF170*, or both *BAF155/BAF170* combined. After 7 days of culture, an analysis of variance (ANOVA) was performed to determine differences in mean nuclei numbers and morphological blastocyst percentages across the three groups. No significant difference was seen between means of treatment groups vs. both control groups. Significant differences were seen between siRNA and Non-Injected groups as well as Non-Injected and Scramble RNA groups. However this indicates that loss of *BAF155*, *BAF170*, or a combination of the two transcripts is not the driving force of the significant differences, rather the microinjection itself caused the differences.

The third study examined the process by which BAF155 and BAF170 proteins are imported from the cytoplasm into the nucleus. It was hypothesized that karyopherin α 7 (KPNA7), a nuclear importer known to be prevalent in the porcine oocyte and early embryo, is the main importer of both subunits. A dominant-negative KPNA7 construct missing the importin beta binding (IBB) domain was microinjected into parthenogenetically activated embryos to outcompete competent wild-type KPNA7. No change in protein localization was seen at the 4-cell stage of development (48 hours post-injection) for either BAF155 or BAF170. To reinforce these results, an RNAi targeting *KPNA7* was also microinjected into parthenogenetically activated embryos. Again, no change was shown in protein localization at the 4-cell stage (48 hours post-injection), indicating that KPNA7 was not the main nuclear importer of either BAF155 or BAF170.

Further study is necessary to determine transcript abundance and the mechanism of nuclear import of both BAF155 and BAF170.

CHAPTER 1: REVIEW OF LITERATURE

1.1 Significance

The creation of viable *in vitro* derived embryos is vital to several technologies within the areas of both agriculture and human health. It is well-known that *in vitro* techniques are subversive to embryonic development across species, with some diseases and disorders more prevalent in individuals generated by these methods (Lu et al. 2013). Errors in the mediation of chromatin remodeling are theorized to be one of the causes of both a higher prevalence of certain disorders such as Parkinson's disease, Prader-Willi syndrome, and α-thalassemia as well as reduced developmental rates and/or arrest at certain stages of preimplantation embryo development (Lu et al. 2013; Snyder et al. 2013). The available literature covers an expansive list of approaches applied to investigate how chromatin remodeling factors affect *in vitro* derived embryos. Examples of these approaches are: *in vitro* fertilization, embryo culture, immunocytochemical staining, qPCR, and RNA interference (RNAi) assays. The literature presents and discusses these technologies in many contexts. Here, the focus will be on how these approaches (technologies) may be applied to furthering our understanding of how chromatin remodeling pathways affect the development of human disease as well as the viability of *in vitro* derived embryos in humans and animals alike.

1.2 Chromatin Structure

The packaging of deoxyribonucleic acid (DNA) is an efficient and orderly process as the approximately 2 meters of DNA present in each mammalian cell must be compacted into a 5μm wide nucleus. The way DNA is structured within the nucleus not only allows for its storage in such a small space but also affects the rate at which it is transcribed. The classic "double helix"

is the most basic framework of DNA. It consists of two sugar-phosphate backbones that twist around one another in a cork screw fashion. Matched pairs of either adenine bound to thymine or cytosine bound to guanine connect these two sugar-phosphate backbones, forming the familiar ladder-like double helical shape (Annunziato, 2008). However, DNA is rarely present in this simple structure. Most of the time, it is packaged into functional units called nucleosomes in order to conserve space within the nucleus. Nucleosomes are formed when eight histone proteins bind together to form an octamer, allowing 146 base pairs to wrap around the structure. With the addition of a single H1 histone protein, a chromatosome is formed. The nucleosomes fold up around one another, connected by DNA that runs between nucleosomes (termed "linker DNA"), and form a stretch containing hundreds of thousands of nucleosomes (Figure 1.).
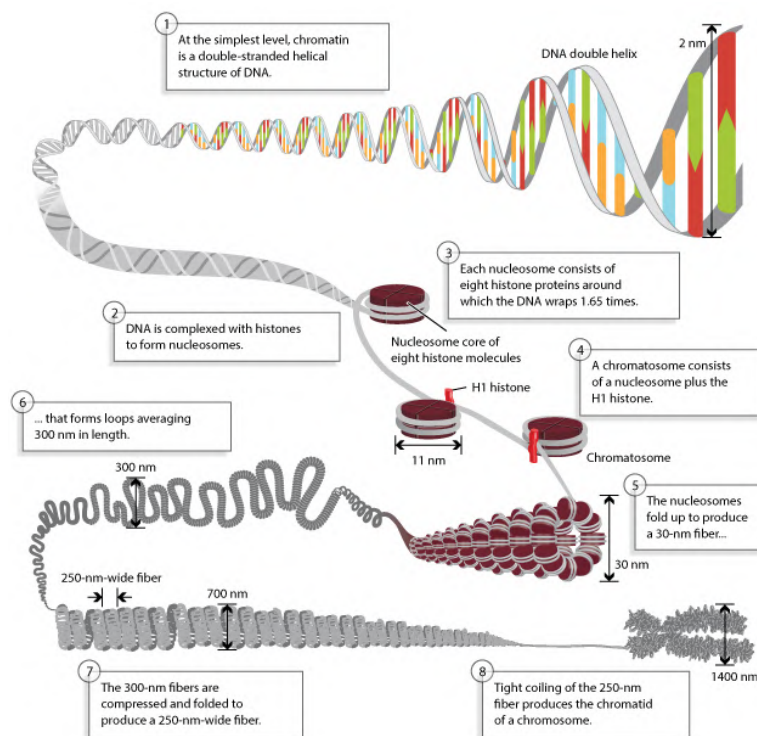
Figure 1: The packaging of DNA from the basic double helix to condensed heterochromatin (Annunziato, 2008).

This stretch of DNA/nucleosomes is coiled twice more before eventually forming the chromatid structure. Nucleosomes are the functional unit of chromatin. Chromatin appears in two forms: euchromatin and heterochromatin (Annunziato, 2008). Euchromatin is loosely packed within the cell and allows for higher rates of transcription. The euchromatin structure is represented by nucleosomes connected by DNA before they are wound into the initial 30nm filament. Under electron microscopy, euchromatin appears as beads along a string, with the beads being the nucleosomes and the string being unwound DNA. By comparison, heterochromatin is more densely packed. In this structure, the nucleosomes add their last histone protein (H1) (Annunziato, 2008). Now chromatosomes, they are able to bind tightly to one another in a dense filament. The DNA contained within this filament is effectively "silenced" as it is unable to be accessed by the DNA polymerases necessary to begin the process of transcription.

1.3 Covalent Modification

Modification of the histone proteins and DNA is one of the driving forces for what is now referred to as epigenetics. Most commonly known for causing diseases and disorders are mutations to the genetic code itself, or alterations in the sequence of paired nucleotides. In contrast, epigenetic changes are not caused by alterations in the DNA sequence, but are modifications of epigenetic marks that might cause changes in gene expression (epimutations). Histone structure may be epigenetically modified in order to allow for specific sections of the DNA to be accessible or inaccessible to DNA polymerases and other transcription factors, thus activating or repressing rates of transcription. The process of modifying chromatin structure to make it more or less accessible to transcriptional proteins is commonly referred to as "chromatin remodeling".

In the case of mammalian histone acetylation, histones may have an acetyl group transferred onto the N-terminus of their lysine residues, effectively removing positive charges and thus loosening the bond between histone protein and DNA allowing for free transcription (reviewed by Grunstein 1997). For example, the entirety of the second X chromosome in females is silenced due to a lack of acetylation on histone H4 (Jeppesen & Turner 1993). In contrast, in non-mammalian species, as in Drosophilia, acetylation of the histone H4 protein at lysine-12 corresponds directly with the presence of heterochromatin indicating that histone acetylation works in this case to silence as opposed to activate transcription (Turner et al. 1992).

Acetylation is effected by Histone Acetyltransferases (HAT) and may be reversed via Histone Deacetylases (HDACs). The downregulation of HDAC1 through treatment with oxamflatin in porcine somatic cell nuclear transfer (SCNT) embryos has been shown to result in hyperacetylation of histone H3 at lysine-9 and subsequently increase embryo vigor (Hou et al. 2014). During deacetylation, the acetyl group is removed from where it was transfixed upon the N-terminus of the lysine residue, returning the positive charge and consequently, the strong interaction between histone protein and DNA. This tight arrangement between histone protein and DNA hinders DNA polymerases and other transcription factors from binding to DNA, leading to a repression of transcription. It has been found that HDAC1 and HDAC2 play a pivotal role in cell proliferation and S-phase progression. Unsurprisingly, many cancers have shown a deregulation of HDAC1 and HDAC2 leading to growth of tumors (Segré et al. 2011).

DNA methylation is another covalent modification that plays its own part in epigenetic modifications. The addition of a methyl group (CH_3) onto the 5-carbon of cytosine is amongst the most common occurrences of DNA methylation, although it may also occur on other DNA bases. The modification upon the cytosine is mediated by DNA methyltransferases (DNMTs)

which results in 5-methylcytosine. This methyl group projects into the space where the backbones of DNA are furthest apart, otherwise known as the major groove, and prevents transcription. DNA binding proteins, such as those necessary for transcription, bind most readily to these major grooves and are effectively prevented from doing so by the protruding methyl groups during DNA methylation (Razin and Cedar, 1991). Thus, an increase of DNA methylation, specifically on gene promotors, correlates heavily with low or no transcriptional activity. It has been shown in mice that lack of DMNT causes embryos to die in the early stages of development (Suzuki and Bird, 2008).

Proteins involved in the methylation of DNA have been found to bind to proteins involved in the deacetylation of histones, producing a combinatory inhibitory effect on transcription. In germ cells, despite DNA methylation being in stable state, demethylation may take place. This process is not entirely understood, although may be explained with the action of DNA deaminases. When deaminases remove a methylated amino acid, they create a mismatch of what must be repaired. The new amino acid inserted during repair is not methylated, thus demethylation occurs (Razin and Cedar, 1991).

Similar to DNA, histones may also be methylated. While DNA methylation is often a stable and static process, histone methylation changes rapidly depending upon the stage of the cell cycle. Methylation occurs on the lysine and arginine residues of the histones in a mono-, dimethylated fashion, in the case of arginine, or also trimethylated in the case of lysine (Bridi & Abel, 2013). The consequences of histone methylation on the transcriptional accessibility of the chromatin seem to be largely dependent on the location and the degree of methylation (mono-, di-, tri-). For example, and in general, methylation events occurring on the K4, K36, and K79 of histone H3 were found to increase transcriptional activity. Methylation on the K9 of histone H3 and K20 of

histone H4, however, were found to mark silenced or reduced transcriptional activity (Ng et al., 2009).

Phosphorylation by kinases and dephosphorylation by phosphatases constitute yet another mechanism by which histones may be modified. These processes may occur at all four histone tails on their serine, threonine, and tyrosine residues. The phosphorylation of these histone tails affects several systems within the cell, including: DNA damage repair, apoptosis, transcriptional regulation, and chromatin compaction (Rossetto et al. 2012). Here, I will focus on the latter two of these. It has been shown that many of the events causing phosphorylation of histones control the transcriptional activation of proliferative genes, such as epidermal growth factor (EGF) responsive genes (Rossetto et al. 2012). Known to be phosphorylated on multiple residues, the H1 linker histone aids in the stabilization of nucleosomes into a chromatosome. Phosphorylation of this H1 linker histone has been suggested as a possible mechanism for the chromatin relaxation to enable transcription (Metzger et al. 2008).

The phosphorylation on the threonine-11 and serine-10 residues of histone H3's tail stimulates transcription of such cell cycle regulators as cyclin B and cdk1, by way of increasing H3K9 and H3K14 acetylation (Clements et al. 2003). Thus, in some instances, phosphorylation indirectly affects activation of certain genes through the regulation acetylation. Interestingly, studies suggest that not only does phosphorylation affect rates of acetylation, but also methylation on the N-terminus of H3. The phosphorylation of H3 specifically regulates gene transcription and, subsequently, expression in this manner (Rossetto et al. 2012). While all four histone proteins have been shown to play a role in either condensation or decondensation of chromatin, H3 shows the highest correlation with phosphorylation and chromatin condensation. The threonine-3 (T3), serine-10 (S10), threonine-11 (T11), and serine-28 (S28) residues of histone H3 can all be

phosphorylated. However, H3S10 phosphorylation during mitosis and meiosis is associated with chromatin compaction (Rossetto et al. 2012).

1.4 Non-Covalent Modifications

Another way the regulation of chromatin remodeling occurs is through the use of ATP dependent chromatin remodeling complexes. These protein complexes all contain an ATPase derived of the SNF2 protein superfamily that provides the energy necessary for their active chromatin remodeling power (Vignali et al. 2000). ATP hydrolysis is the mechanism by which phosphoanhydride bonds are split to release concentrated energy from ATP molecules. The structure of chromatin remodeling protein complexes is highly conserved, however, the complexity of chromatin remodeling complexes increases in higher eukaryotes. These complexes have been organized into five groups, with slight variations in structure and mechanism: SWI/SNF, ISWI (imitation SWI), Mi-2, INO80, and SWIR1. The SWI/SNF chromatin remodeling complex will be discussed in more detail below (Section 1.5).

The second group of chromatin remodeling complexes is ISWI, or imitation SWI. Complexes belonging to this group are smaller and contain fewer subunits than the complexes belonging to the SWI/SNF group. Most studied members of this group include: ACF (ATP-utilizing chromatin remodeling and assembling factor), NURF (nucleosome remodeling factor), and CHRAC (chromatin accessibility complex). The ATPase ISWI is present in all of these complexes and is homologous to the SNF2-type ATPase in the SWI/SNF group. The ISWI ATPase is nucleosome dependent and requires a small sequence on the histone 4 (H4) tail for its activity. In contrast, this is not the case in either SWI/SNF or Mi-2 complexes (Vignali et al. 2000). Complexes in the ISWI group contain SANT and SLIDE domains that allow for the

binding of DNA and remodeling of chromatin. The SANT domain has a strong homology with Myb-related proteins and plays a role in covalent modification of histones via histone acetylation and deacetylation (Boyer et al. 2004). SANT is arranged with three alpha helices organized in a helix-turn-helix motif. Each helix contains a large aromatic subunit that, when present as a triad, creates a hydrophobic core necessary for protein folding. This structure is nearly identical to the Myb-related proteins (Aasland et al. 1996). The three Myb proteins (a-myb, b-myb, and c-myb) bind DNA with matching sequence specificities. These sequences encode proteins which activate transcription (Oh and Premkumar, 1999). However, studies have shown that SANT is minimally sensitive to DNA, making it a poor candidate for the binding component of ISWI complexes. A similar domain present, SLIDE (SANT-like ISWI domain), shows strong interactions with DNA, and the loss of SLIDE results in an inability to bind to target DNA sequences. Thus, SLIDE is necessary for DNA binding of the complexes within the ISWI group. All studied eukaryotes, from yeast to humans, contain ISWI complexes although their abundance is highly variable (Boyer et al. 2004).

Best categorized of the third group, Mi-2, is the NuRD (Nucleosome Remodeling Deacetylase) complex. This nucleosome remodeling complex contains the Swi2/Snf2 homologous CHD4 ATPase. It also possesses two PhD zinc finger motifs and two chromodomains (Vignali et al. 2000). The structure of PhD zinc fingers is highly variable (Laity et al. 2001). PhD zinc finger motifs recognize and bind to the methylated and, to a lesser extent, acetylated N-terminal lysine residues on histone 3 (H3) (Sanchez, 2011). Chromodomains consist of a three stranded beta sheet packed against a C-terminal alpha helix. They assist with the assembly of remodeling complexes onto chromatin, specifically by recognizing methylated lysine residues on histone 3 (H3) ("Chromatin Protein Domain."). NuRD complexes also contain the methyl-CPG binding

protein 3 (MBD3). Instead of binding to methylated histone H3, MBD3 binds to hydroxymethylated DNA (Yildirim, 2011). The complexes of the Mi-2 group work as both deacetylases and chromatin remodelers by utilizing their Mi-2 and CHD subunits (Vignali et al. 2000).

Last of the five groups, INO80 and SWR1, have been described more recently and are characterized by a split core ATPase domain (Figure 2.; Boa and Shen, 2007) and the presence of Rvb proteins.
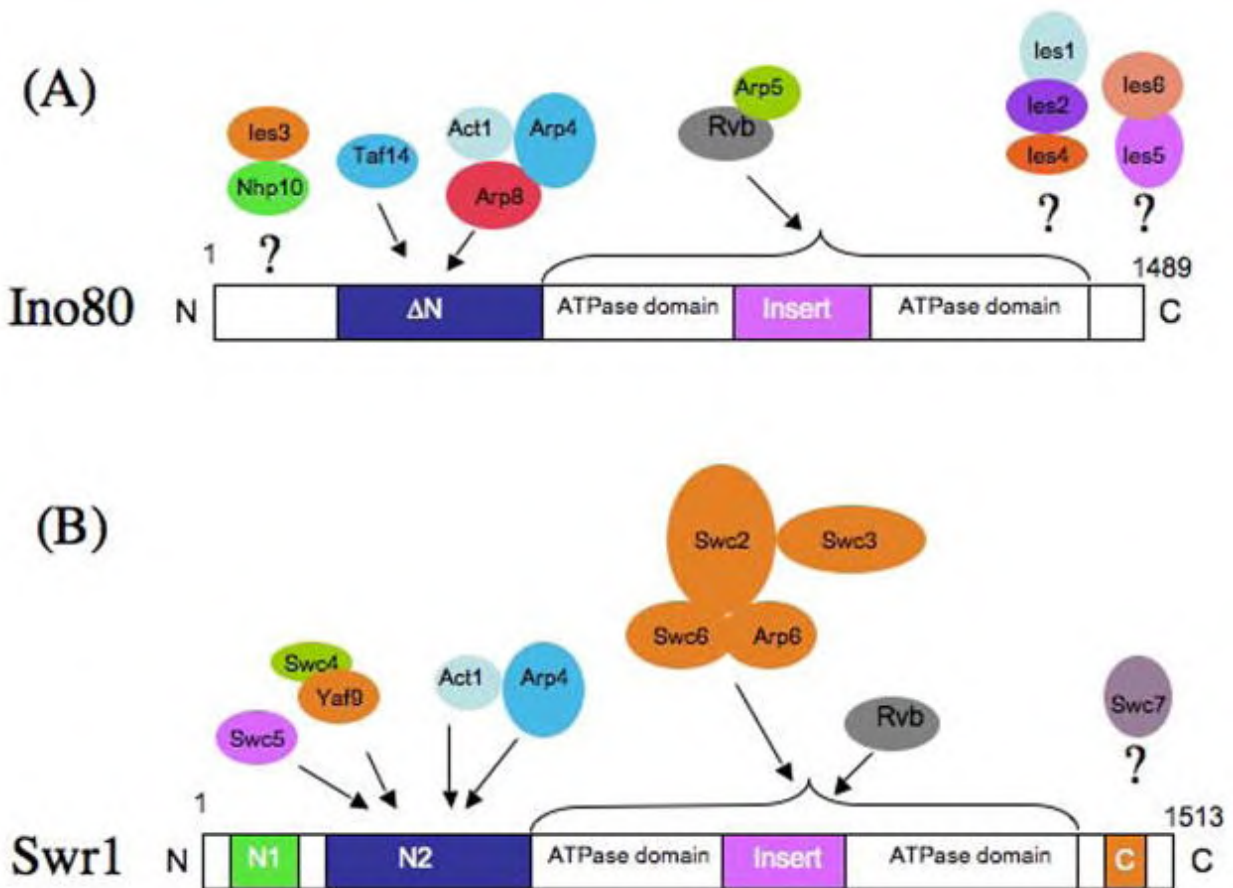
Figure 2: Configuration of the split ATPase domain with an insert in the middle of each domain (Bao and Shen, 2007).

Rvb proteins associate closely with another subunit within the INO80 complex, Arp5, to regulate the activity of the complex (Bao and Shen, 2007). Actin-related protein 5 (Arp5) is an essential subunit to the INO80 complex. The loss of Arp5 disrupts DNA binding capabilities, nucleosomal movement by INO80, and ATPase efficiency (Shen et al. 2003). Complexes within the SWR1 group include the same Rvb proteins, but not Arp5 (see Figure 2), suggesting that there may be a different regulating subunit with which the Rvb proteins associate (Bao and Shen, 2007).

1.4.1 SWI/SNF Complexes

The SWI/SNF group includes the ySWI/SNF (yeast), Brahma (human and Drosophilia), RC (yeast), and BRG1 (human) complexes. These complexes all utilize an ATPase of the SNF2-type, BRG1 or BRM. The ATPase utilizes energy from ATP hydrolysis. Complexes within this family also contain a bromodomain at their C-terminal region (Vignali et al. 2000). The bromodomain includes four alpha helices (αZ, αA, αB, and αC) and two loops (ZA, and BC) which diverge from one another. These four alpha helices, flanked by the two divergent loops, surround an inner hydrophobic pocket where acetylated lysine (Kac) is able to bind. Bromodomains specifically bind to the N-terminus of an acetylated Lys 4 on histone protein 3 (H3) (Fujisawa and Filippokapoulos, 2017). This binding allows for the complex to boast a certain level of specificity to which DNA it binds and, subsequently, remodels. SWI/SNF complexes will be described in more detail below.

Although all SWI/SNf complexes remodel chromatin, distinct complexes within the SWI/SNF group are found in different species, affect different genes, or occur during different developmental stages. Each complex is made up of an ATPase, core subunits, and accessory subunits (see Table 1).

Table 1: Specific subunits of mammalian SWI/SNF complexes and their importance (Modified from Weissman and Knudsen, 2009).

Subunit	Gene(s)	Role	Phenotypes
BRG1	*SMARCA4*	ATPase	KO increases lung tumor development in mice (Marquez-Vilendrer et al. 2016)
BRM	*SMARCA2*	ATPase	KO increases lung tumor development in mice (Marquez-Vilendrer et al. 2016)
SNF5	*SMARCB1*	Core	KO induces malignant rhapdoid/lung tumors in mice (~10 weeks) (Marquez-Vilendrer et al. 2016)
BAF155	*SMARCC1*	Core	Knockout causes loss of pluripotency in murine embryonic stem cells (Ho et al. 2009)
BAF170	*SMARCC2*	Core	Mutations cause intellectual and developmental disorder (Machol et al. 2018)
BAF45 (a-d)	*PHF10, DPF1, DPF2, DPF3*	Accessory	
BAF53 (a,b)	*ACTL6A, ACTL6B*	Accessory	
BAF57	*SMARCE1*	Accessory	Depleted in 10-14% of breast cancer cases (reviewed by Kadoch and Crabtree, 2015)
BAF60 (a-c)	*SMARCD1, SMARCD2, SMARCD3*	Accessory	
BAF180	*PBRM1*	Accessory	KO causes abnormalities in the cardiac muscles and placental tissues (de la Serna et al. 2006; Xu et al. 2012)
BAF200	*ARID2*	Accessory	
BAF250 (a,b)	*ARID1A, ARID1B*	Accessory	ARID1B Haploinsufficiency causes intellectual disability (Santen et al 2010)
BRD7	*BP75, NAG4, CELTIX1*	Accessory	
BRD9	*PRO9856, LAVS3040*	Accessory	
Actin	*ACTB*	Accessory	

KO - Knockout

SWI/SNF complexes were first discovered in *Saccharomyces cerevisiae* and were named for the switching mating types of yeast (SWI) and sucrose non-fermenting (SNF) (Tang et al. 2010). In mammals, SWI/SNF complexes have two major biochemical configurations; the BAF and PBAF complexes (see Figure 3).
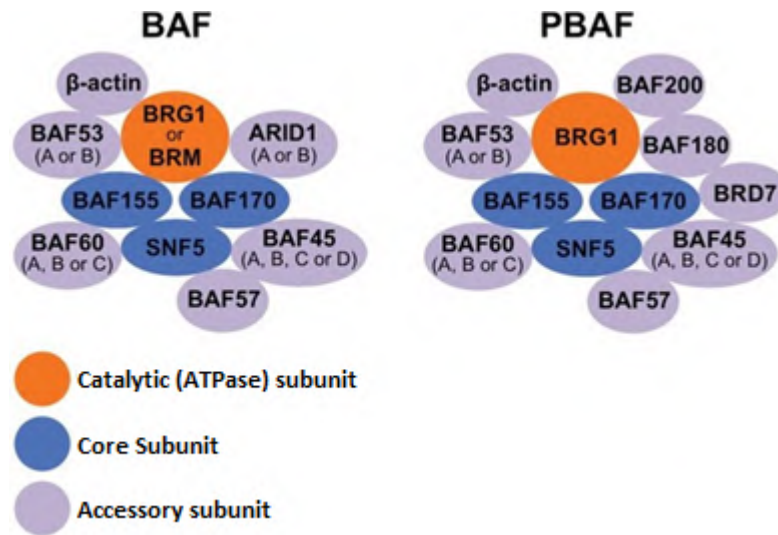
Figure 3: Differences between biochemical configuration of BAF and PBAF complexes subunits (Oike et al. 2014).

First of these, the BAF chromatin remodeling complexes have either a BRG1 or BRM subunit for an ATPase, while the PBAF complexes only incorporate BRG1 as the ATPase subunit. The two SWI/SNF compositions are found during different processes. BAF complexes are important to both embryonic stem cell pluripotency and early embryogenesis while also having implications in cancer as the complex is frequently mutated in long-term cell lines associated with cancer (Hodges et al. 2014). PBAF complexes are involved in cellular differentiation and are possibly an important cell-identity regulator (reviewed by Clapier and Cairns, 2009). PBAF complexes also have important implications in genomic integrity during mitosis (Hodges et al. 2014). There are three subunits of significance in the PBAF subunits, these being: ARID2, BAF180, and BRD7. ARID2 (AT-rich interactive domain 2) is also referred to as BAF200. These subunits are not present in BAF complexes and are unique to the PBAF complexes (see Figure 3).

A third biochemically distinct complex, termed GBAF, has been discovered recently and might be less important for chromatin remodeling than the two previously discussed. Contained within this SWI/SNF subcomplex are two unique subunits: GLTSCR1 (glioma tumor suppressor candidate region gene 1) and GLTSCR1L (GLTSCR1-like), which replace ARID1A/B (BAF) or ARID2 (PBAF). In addition to these novel subunits, the GBAF complexes also contain BRD9, BAF155, BAF60, SS18, BAF53, and BRG1/BRM subunits while lacking SNF5. Despite the differences in composition, the GBAF complexes show ATPase activity and chromatin affinity comparable to BAF complexes (Alpsoy and Dykhuizen, 2018).

Studies *in vitro* have given insight into the mechanisms by which SWI/SNF complexes remodel chromatin to allow for control of gene transcription. SWI/SNF alters the rotational phasing of the DNA around the nucleosome (Vignali et al. 2010). The DNA segments closest to the histone are the least accessible to transcription factors and thus, transcription for those segments is repressed. Taking into account DNA's helical structure, the segments of the helices closest to the histone proteins are inaccessible for transcription while the remaining segments are more accessible. Rotational phasing refers to the rotation of the DNA helix. If the helix is turned, new sections of DNA are exposed and thus their rate of transcription is increased (See Figure 4).
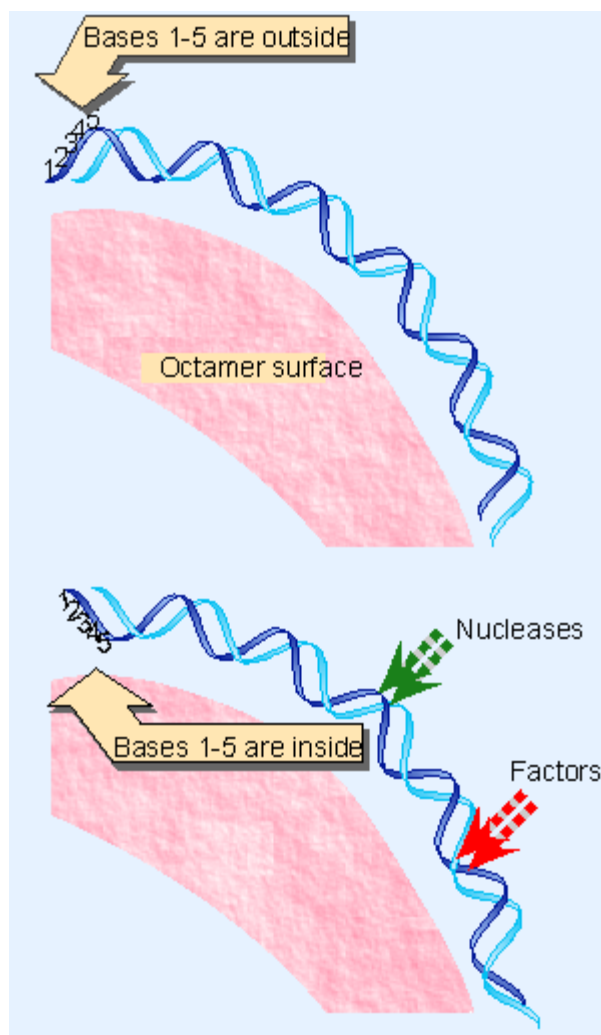
Figure 4: Rotational phasing of DNA determines the exposed face of DNA for transcription.
(Lewin, 1999)

SWI/SNF complexes are able to modify said rotational phasing of the DNA helix, control which segments of the helix are accessible for transcription, and consequently affect gene transcription.

Disruptions in the composition or abundance of particular SWI/SNF complexes have implications for many diseases, syndromes, and disorders. Well studied is SWI/SNF's role in tumorigenesis as SWI/SNF complexes have widespread functions in the suppression of cancer.

1.4.1.1 ATPases

The complex's ATPases exhibit different abilities in the activation of genes associated with proliferation or differentiation. The two ATPases, BRG1 (SMARCA4) and BRM (SMARCA2), share 74% homology and possess similar biochemical activities *in vitro* (Trotter and Archer, 2008). BRG1 includes a C-terminal bromodomain, which recognizes and binds acetylated lysine on the histone 3 (H3) and histone 4 (H4) tails. BRG1 also contains an AT-hook motif, which binds to AT-rich domains such as accessory ARID subunits. Less characterized are BRG1's N-terminal QLK, BRK, and HAS domains (Fan et al., 2005; Khavari et al., 1993). Although the BRM subunit shares much of its structure with BRG1, Ankyrin repeat proteins help mediate different DNA binding capabilities. These Ankyrin repeat proteins contain a helix-turn-helix structural motif at each repeat and function exclusively to mediate protein-to-protein interactions (Li et al. 2006).

The core ATPase subunits BRG1 (SMARCA4) and BRM (SMARCA2) have been shown to have different developmental requirements dependent on the stage of embryonic development. In a murine model, the loss of Brg1 at the stage of embryonic gastrulation leads to an increase in apoptosis and subsequent embryo death. Brg1 tamoxifen-inducible knockout embryos exhibited a phenotype of retarded growth progressing until Day 10.5 when resorption occurs. This study suggests that Brg1 has a role in both proliferation and the suppression of apoptotic factors; such as p53 (Singh et al. 2016). Knockdown of Brg1 causes an increase in the levels of Oct4 and Nanog, which have well-known implications in the maintenance of pluripotency. This increase in Oct4 and Nanog leads to a differentiation of embryonic stem cells and a loss of pluripotency (Singhal et al. 2010). BRG1 was found to have lower transcript levels in the metaphase II (MII) stage, compared to germinal vesicle (GV) porcine oocytes. *BRG1* transcript abundance returns to

and stabilizes at GV levels starting with 2-cell stage porcine embryos. *BRM* shows a decrease in transcript abundance, from the GV stage of porcine oocytes, to the MII stage as well. However, *BRM* levels continue to decrease to a minimum abundance at the 8-cell and blastocyst stages in porcine embryos (Magnani and Cabot, 2009). A knockdown of BRM using RNAi microinjection post-fertilization resulted in an arrest in development at the 2-cell stage, indicating that BRM is essential to porcine embryonic development (Magnani and Cabot, 2007). Knockdown of BRG1 in the porcine embryo resulted in arrest of development before the 4-cell stage (Magnani and Cabot, 2009).

Interestingly, and in contrast to the pig (Magnani and Cabot 2007), knockout of Brm in the murine model shows only a slight phenotype of overgrowth in the adult mouse and is not lethal (Kidder et al. 2009). Knockdown of murine *Brm* causes a loss of germline stem cells (He et al. 2014). Knockout of both *Brg1* and *Brm* in the adult mouse has been shown to increase the development of lung cancer (Marquez-Vilendrer, 2016).

1.4.1.2 Accessory Subunits

Loss of particular SWI/SNF proteins, specifically the *Baf47 (Smarcb1)* subunit in the murine model, is known to permit the growth of malignant rhabdoid and lung tumors (Marquez-Vilendrer et al. 2016). Loss of specific subunits also has implications in other diseases and disorders (See Table 1). For example, ARID1B haploinsufficiency is associated with symptoms including severe intellectual disability, speech delay, and agenesis of the corpus callosum (Santen et al. 2012). ARID1A deficiency has a widespread tumorigenic effect in many types of cancer, such as gastric, pancreatic, colon, rectal, childhood neuroblastoma, endometrial, and bladder cancers. The absence of BAF57 has a generally low prevalence in tumor development

with the exception of breast cancer (10-14%). The study of SWI/SNF complexes and their individual subunits aid in a better understanding of the origin of certain diseases (reviewed by Kadoch and Crabtree, 2015).

In mice, the knockout of *Snf5* results in peri-implantation lethality (Guidi et al. 2001). Porcine embryos after a knockdown of SNF5 failed to cleave (Personal communication – Yu-Chun Tseng, Purdue University). The PBAF specific subunit, BAF180, is also critical for embryonic development. *Baf180*-null mouse embryos do not survive past E12.2-E15.5 with abnormalities in the cardiac muscles and placental tissues evident (de la Serna et al. 2006; Xu et al. 2012). Knockout of *Baf57* in mice also leads to an early embryonic lethality (reviewed by Lessard and Crabtree 2010). There are differences in knockout effects between Arid1a and Arid1b*,* with Arid1a knockout mice presenting an embryonic arrest around E6.5, while Arid1b knockout embryonic stem cells lack sufficient pluripotency (Gao et al, 2008; Yan et al, 2008). Differing embryonic requirements as well as the association with disorders or lethality justifies the study of specific SWI/SNF subunits in order to better understand the mechanisms underlying the success of *in vitro* embryo production to other potential improvements thereof.

1.4.1.3 SWI/SNF Scaffolding Subunits

SWI/SNF complexes, in mammals also known as the Brahma or Brahma-related gene 1 (BRG1)-associated factor (BAF) complexes, contain at least 15 subunits whose functions are important to an organism's growth and development (reviewed by Kadoch and Crabtree, 2015). Most notable of these are the core ATPases: either BRG1 or Brahma (BRM), SNF5 (SMARCB1); and the scaffolding subunits: BAF155 (SMARCC1), BAF170 (SMARCC2).

A scaffolding subunit maintains the integrity of the complex, holding all accessory subunits and the ATPase in place for the continuity of the action of the complex. Two of these subunits, BAF155 and BAF170, are present in SWI/SNF complexes (Figure 5; Narayanan et al. 2015).
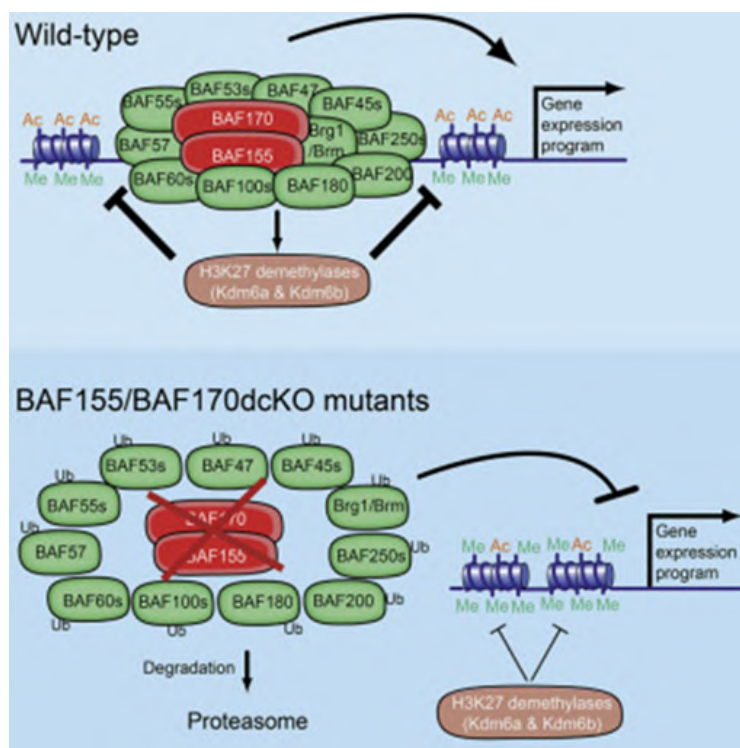
Figure 5: Knockout of both BAF155 and BAF170 causes a disassociation of all other subunits. (Narayanan et al. 2015)

BAF155 and BAF170 form either homodimers with themselves, as seen in SWI/SNF BAF complexes of murine embryonic stem (ES) cells (Ho et al. 2009), or heterodimers with one another (Wang et al. 2016). BAF155 and BAF170 immunodepletion showed that there is preferential homodimerization of BAF155. Most subunits of the SWI/SNF complex are present in a relative stoichiometry of 1:1, however, BAF155 was shown to be present in a 1:1.6 stoichiometry. BAF170, in contrast, is present in 1:1 stoichiometry. This shows a preference for BAF155 to form homodimers over BAF170 (Mashtalir et al. 2018).

Embryonic stem cells are pluripotent, having the ability to divide and differentiate into all embryonic cell lineages. In mice, *Baf155* has importance in the maintenance of ES cell pluripotency. Western blot analysis of nuclear extracts in murine embryonic stem cells shows a presence of Baf155 and an absence of Baf170, indicating that Baf155 forms a homodimer (Ho et al. 2009). In contrast, human embryonic stem cells show a presence of both BAF155 and BAF170, indicating a heterodimeric formation between the subunits (Zhang et al. 2014).

In the murine embryo model, deletion of *Baf155* leads to peri-implantation lethality (Ho et al. 2009). If there is an overexpression of Baf155, an arrest at the blastocyst stage occurs. This may be due to the fact that the amounts of BAF155 and BAF170 control the quantity of BAF57, an important subunit for the interactions between SWI/SNF and transcription factors (Chen & Archer, 2005; reviewed by Lomelí & Castillo-Robles, 2016). However, in the porcine model, both BAF155 and BAF170 are present in the nuclei of early developing embryos (Cabot et al. 2017), similar to human embryonic stem cells (Zhang et al 2014).

Losses of one or both of these subunits have varying degrees of detriment to a developing organism. In murine embryos homozygous for a mutant form of *Baf155*; anencephaly, exencephaly, and developmental delays were found in dissected embryos. This mutant allows for the structural formation of the SWI/SNF complex, but disrupts proliferation and apoptosis within the neural tube. (Harmacek et al. 2014). *Baf170* knockout mice show an increase in the thickness of their developing neocortex, while overexpression shows a reduction of neocortex (Tuoc et al. 2013). In addition, *Baf170* knockout mice exhibit an increased birth weight phenotype while overexpression of *Baf170* leads to reduced birth weights in mice (Tuoc et al. 2013). Instances of a natural deletion or mutation of BAF170 in humans lead to disorders that effect both intellectual and developmental processes. When analyzing, individuals exhibiting

specific intellectual and developmental disability symptoms indicative of syndromes like Coffin-Siris and Nicolaides-Baraitser, such as: speech impairment, seizures, feeding difficulty, behavior disorder, and palate abnormalities, eight of fifteen children were found to have mutations in their BAF170 subunit. This indicates a correlation between a syndrome like Coffin-Siris or Nicolaides-Baraitser and mutations in the BAF170 subunit (Machol et al. 2018).

1.5 Nuclear Trafficking/Nuclear Pore Complex

The transport of proteins between the cytoplasm and the nucleoplasm is an essential process to the cell. The mechanism behind this shuttle between cellular compartments is regulated depending upon the size and characteristics of the molecule. Diffusion is a possible mode of travel for molecules less than 50 kDa.

Import into the nucleus begins with binding of karyopherin α to the nuclear localization sequence (NLS), a series of specific amino acids on the potential cargo protein that "tags" it for import into the nucleus. This binding to karyopherin α occurs in the cytoplasm. The karyopherin import complex contains two proteins: karyopherin α (KPNA) and karyopherin β (KPNB). Both proteins are required for the binding and subsequent transmission of the cargo through the nuclear envelope. KPNA binds directly to the nuclear localization sequence while KPNB assists KPNA in binding to the cargo and the nuclear envelope. Both proteins, already bound to the NLS of the cargo, must bind to the proteins of the nuclear pore complex (NPC) before translocation. After movement through the nuclear envelope, the KPNA/KPNB/Cargo trimer dissociates upon binding to the GTP (active) form of Ran (see Figure 6).
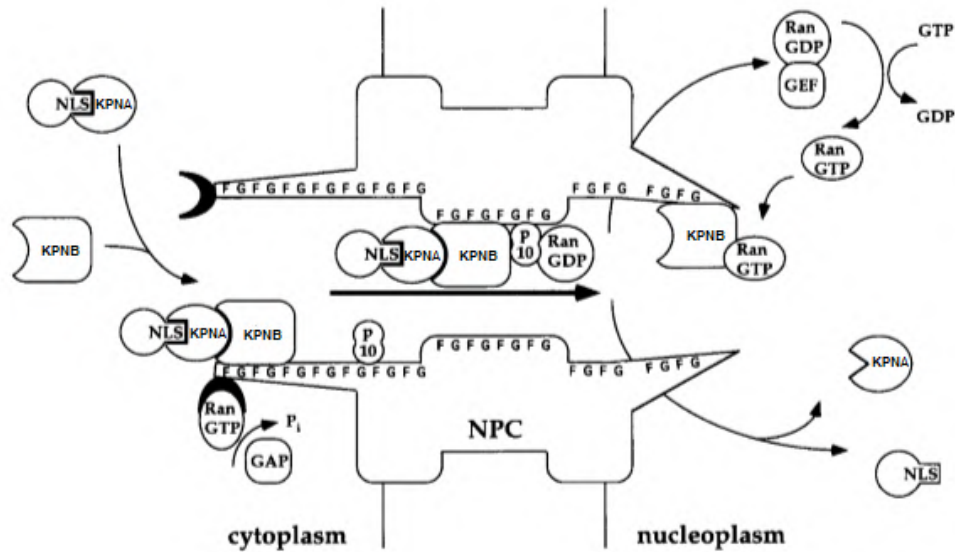
Figure 6: Schematic of nuclear import through nuclear pore complex mediated by the karyopherin α/karyopherin β system (modified from Schlensted, 1999).

The GTP form of Ran is found both in the nucleoplasm and cytoplasm while the GDP form is concentrated in the nucleoplasm. The GTP form of Ran is necessary for the export of molecules, such as RNA, from the nucleoplasm to the cytoplasm in a reverse process to import (Wente and Rout, 2010; Schlensted,1999). KPNA and KPNB are then exported back into the cytoplasm for binding to another cargo.

1.5.1 Nuclear Import

Large protein subunits, e.g. those necessary for the assembly of SWI/SNF complexes must be able to enter the nucleus to enable action on chromatin. Because SWI/SNF complexes are extremely large (1.1-1.3 MDa), it is likely that individual subunits are actively imported through the NPC for the SWI/SNF complex to be assembled within the nucleus. The import of SWI/SNF subunits may be mediated by karyopherin α/β heterodimers. Karyopherins usually bind directly to their own substrate, but sometimes require an adaptor protein. Karyopherin α (KPNA)

recognizes and binds to both karyopherin β (KPNB) and the nuclear localization sequence (NLS) on many proteins. Nuclear localization sequences contain a string of specific amino acid residues necessary for recognition, often lysine heavy. KPNA forms a heterodimeric domain with KPNB, which increases the binding affinity for NLS, compared to the weak binding affinity characterized by KPNA alone. Once the cargo-carrying heterodimer enters the nucleus, Ran-GTP mediates the dissociation of the heterodimer and the release of the cargo into the nucleus (Blobel and Chook, 2001).

Six karyopherin α shuttle proteins, also referred to as importins, have been identified in humans. These are divided into three subfamilies with the proteins of each family sharing ~85% sequence identity with one another. The first subfamily contains KPNA2, the second contains KPNA3 and KPNA4, and the third contains KPNA1, KPNA5, and KPNA6. A seventh subtype of karyopherin α, KPNA7, was identified in porcine and bovine tissues. Karyopherin α7 (KPNA7), is the most divergent shuttle protein of the importin α family. All karyopherin α proteins, including KPNA7, contain an Importin β binding (IBB) domain that binds very strongly to karyopherin β. Strikingly, in porcine embryos KPNA7 has shown nuclear localization in contrast to the most homologous member of the karyopherin α family, KPNA2, which is cytoplasmically localized (Cabot et al. 2012). This may be due to the evidence presented that KPNA7 binds karyopherin β at a much higher affinity than other importin α family members, resulting in an inefficient release of KPNA7 from the nuclear localization sequence. This causes an increase in nuclear retention of KPNA7 (Kelley et al. 2010). *KPNA7* is highly abundant in the porcine germinal vesicle (GV) and MII oocytes but low in later stages of embryo development, such as blastocysts. RNAi knockdown of *KPNA7* in porcine embryos caused a significant decrease in nuclei number at Day 6 post injection when compared with non-injected and scramble injected

control embryos (Wang et al. 2012). KPNA7 was found to import BRD7 in the porcine embryo (Crodian et al. 2019). Similarly, the bovine model shows a high expression of *KPNA7* in the germinal vesicle and MII oocyte as well as pronuclear and 2-cell stage embryos with a sharp decrease in transcript levels in the blastocyst stage. RNAi knockdown performed in the bovine embryo greatly reduced embryo development to the 8-cell and 16-cell stage when compared to non-injected and scramble injected embryos (Tejomurtula, 2009). These reports indicate that KPNA7 is necessary to the preimplantation development of both bovine and porcine embryos.

1.6 Fertilization/Activation

The process of fertilization has requirements of both the spermatozoa and the oocyte. The sperm goes through a process of capacitation, movement through the cumulus cells, an acrosomal reaction, and finally a joining to and penetration of the oocyte's plasma membrane. Ejaculated sperm must pass through the female reproductive tract successfully to become capacitated and fertilize an oocyte. Once the sperm reach the female reproduction tract, motility is attained through exposure to an alkaline environment. Capacitation entails the removal of seminal plasma proteins and carbohydrates acquired in the epididymis. Thereafter, sperm attain the hyperactive movement necessary to push through the cumulus complex surrounding an oocyte. This movement is slower, whip-like, with a large amplitude while pre-capacitation the sperm move in a fast, sinusoidal fashion, with a high amplitude (Tienthai et al. 2003).

Alkalinization increases intracellular Ca^{2+}. Hyaluronidase bound on the surface membrane of the sperm head helps digest the intracellular matrix of hyaluronic acid between cumulus cells. Only capacitated sperm are able to successfully undergo an acrosomal reaction. This process occurs in the oviduct (Tienthai et al. 2003). Once the sperm is capacitated, hyperactivity pushes the head

of the sperm through the cumulus cell complex and into contact with the zona pellucida (ZP). The zona pellucida contains three proteins (ZP1, ZP2, ZP3). The release of the acrosomal enzymes is due to alkalization, binding to ZP3, and an increase in intracellular Ca^{2+}. After the acrosomal reaction, the sperm binds to ZP2, penetrates the zona pellucida, enters the perivitelline space (Burken and Miller, 2002), and subsequently binds to the oocyte's plasma membrane (Bianchi et al. 2014). After fusion of sperm and oocyte, the spermatazoa's tail becomes immotile and is taken into the oocyte along with the sperm head. The early embryo then goes through a membrane hyperpolarization event, effectively preventing additional sperm from binding to the plasma membrane. This hyperpolarization prevents polyspermy in some species. Approximately 15 seconds after this hyperpolarization, transient Ca^{2+} waves begin. This increase of Ca^{2+} can be stimulated artificially when oocytes are placed in a Ca^{2+} rich medium, and e.g. are treated with electrical pulses (Kharch and Birade, 2012). In mammals, the Ca^{2+} release starts at the point of sperm fusion and moves across the early embryo in repeating waves, referred to as oscillations. These Ca^{2+} oscillations result in the resumption of meiosis. Cortical granules containing glycoproteins and specialized enzymes move from the golgi apparatus to the plasma membrane where they release their contents. This results in the 'zona reaction' which hardens the zona pellucida and is a secondary block to polyspermy (Machaty et al. 2017).

1.7 Zygotic Genome Activation (ZGA)

There is an important switch in supply of RNA from maternal to zygotic transcription termed the zygotic genome activation (ZGA). Oocytes are large cells and contain a high abundance of maternal mRNA and proteins for the developing oocyte and early embryo. Prior to the onset of ZGA, the zygote has been transcriptionally silenced while it is developing utilizing maternal RNA. As the developing embryo begins to divide, there is no cell growth (Jukam et al. 2017). In

order for ZGA to occur, both maternal RNA must be degraded and the repression of zygotic transcription must be stopped. Maternal mRNAs are necessary for oocyte maturation and early embryogenesis but may become deleterious or, at the very least, unnecessary, during later stages of embryogenesis (Kanka et al. 2009). This change in transcription control is of importance as the stage of ZGA is the first glimpse into an embryo's developmental competency (Lee et al. 2014; Svoboda, 2017). In the mouse, the embryo is supplied with all of the maternal RNA necessary for development to 2-cell stage (Svoboda, 2017). In the mouse, it has been shown that ZGA is completed through two transient transcriptional "waves". This is considered the earliest ZGA in all vertebrates. In the porcine embryo, this ZGA occurs at the 4-cell stage (Lee et al. 2013; see Table 2). Porcine embryos typically undergo a long 4-cell stage (more than 48 hours) for reasons unknown presently.

Table 2: Differences in embryonic stages of development between species at the initiation of zygotic genome activation, as well as embryo age at blastocyst development (Lee et al. 2014; Kanka et al. 2009; Jukam et al. 2017).

Species	ZGA	Age at Blastocyst stage
Murine	2-cell	Day 3
Human	4-cell	Day 6-7
Porcine	4-cell	Day 6-7
Bovine	8-cell	Day 8

Chromatin remodeling is of importance to the transcriptional transition during zygotic genome activation as different parts of the genome must be accessible to transcription factors during the time of this event.

CHAPTER 2: MATERIALS AND METHODS

Described here are general procedures used in the specific experiments described in Chapters 3-5. All chemicals were obtained from Sigma Chemicals (Sigma-Aldritch, St. Louis, MO, USA) unless stated otherwise.

2.1 Oocyte Aspiration

A local slaughterhouse donated the porcine ovaries, which were collected each morning, rinsed in warm saline, and transported in an insulated container back to Purdue University. Antral follicles were aspirated manually using 10mL Luer-Lok syringes equipped with 20G needles. Oocytes and cell debris were allowed to settle in the collection tube. Follicular fluid was removed from the settled material and the oocytes/debris were washed in TL-HEPES media (2.0 mM $CaCl_2 x2H_2O$, 114.0 mM NaCl, 3.2 mM KCl, 2.0 mM $NaHCO_3$, 0.4 mM NaH_2PO_4, 10.0 mM Na lactate (60% syrup), 0.5 mM $MgCl_2 x6H_2O$, 10.0 mM HEPES, 2.186 g/L sorbitol, 0.075 g/L penicillin, 0.05 g/L streptomycin, 1 mL/L phenol red (0.5%), 0.2 mM sodium pyruvate, 0.1 g/L PVA). Cumulus-oocyte-complexes (COCs) were recovered and selected by morphology. Oocytes with multiple layers of cumulus cells and a uniform cytoplasm were used for further processing.

2.2 Oocyte Maturation (IVM)

Collected COCs were washed in maturation medium (Tissue Culture Medium 199 (TCM199) containing 0.14% PVA, 10ng/ml epidermal growth factor (EGF), 0.57 mM cysteine, 0.5 IU/ml FSH, 0.5 IU/ml LH, 20 ng/ml LIF (MilliporeSigma, Burlington, MA, USA), 20 ng/ml IGF-1 (Prospec Protein Specialists, East Brunswick, NJ, USA), and 40 ng/ml FGF-2 (PeproTech,

Rocky Hill, NJ, USA)), as previously described (Yuan et al. 2017). Afterward, 50-150 COCs/well were placed in 4-well Nunc dishes containing 500µL maturation medium and overlaid with 500µL of mineral oil. Maturation was performed in a humidified incubator at 39˚C with 5% CO_2 air mixture for 42-44 hours.

2.3 In Vitro Fertilization (IVF)

Five hundred µL of 0.1% hyaluronidase in TL-HEPES medium containing 0.01% poly-vinyl alcohol (PVA) was used to strip matured oocytes of their cumulus cells via vortex for 3 minutes. Oocytes with intact plasma membranes were then fertilized using fresh, extended boar semen, according to an established protocol (Abeydeera et al. 1998). Briefly, fresh extended semen was washed three times in DPBS at a ratio of 1mL to 9mL. The suspension (10mL) was spun at room temperature for 4 minutes at 982 xg. This was repeated three times with the supernatant decanted and the sperm pellet gently resuspended in DPBS between each spin. The final pellet was resuspended in 200µL of mTBM (113.1 mM NaCl, 3.0 mM KCl, 7.5 mM $CaCl_2x2H_2O$, 20.0 mM TRIS, 11.0 mM glucose, 5.0 mM sodium pyruvate). Ten µL of the prepared sperm suspension were added to 90µL of water. Then, 10µL of the first dilution were added to 990µL of water. This second dilution was used to determine an average sperm count: 20µL of the second dilution were loaded onto the hemocytometer, and the individual sperm were counted in each of the four quadrants and averaged. To calculate a final concentration of $5x10^5$ sperm per mL/mTBM, the following formula was used:

(100/average sperm count) = x ; x= µL added for a total of 1000µL of sperm/mTBM mixture

$$(5x10^5 \text{ sperm per mL})$$

Gametes were co-incubated for a total of five hours in mTBM media before *in vitro* culture.

2.4 Parthenogenetic Activation

Cumulus cells were removed from matured oocytes, as described above. These denuded oocytes were rinsed briefly (no longer than 30 seconds) in activation medium (300 mM mannitol, 0.1 mM CaCl$_2$, 0.1 mM MgSO$_4$, 0.5 mM HEPES, 0.01% BSA) to equilibrate and allow oocytes to settle on the bottom of the dish. Oocytes were then transferred to a new dish containing activation medium for electrical stimulation. Oocytes were placed between two platinum electrodes (1mm distance) within the dish connected to an Electrocell Manipulator (BTX, San Diego, CA, USA) (See Figure 7). Careful consideration was given to separate oocytes from one another evenly and to keep oocytes from touching either platinum electrode. Two DC pulses of 1.2 kV cm^{-1} for 40 µs, 70 µs apart were used to activate the oocytes. Activated embryos were then placed in a dish of HEPES buffered media until all oocytes were activated. Thereafter, activated oocytes were placed in PZM3 media for subsequent *in vitro* culture (See 2.5).
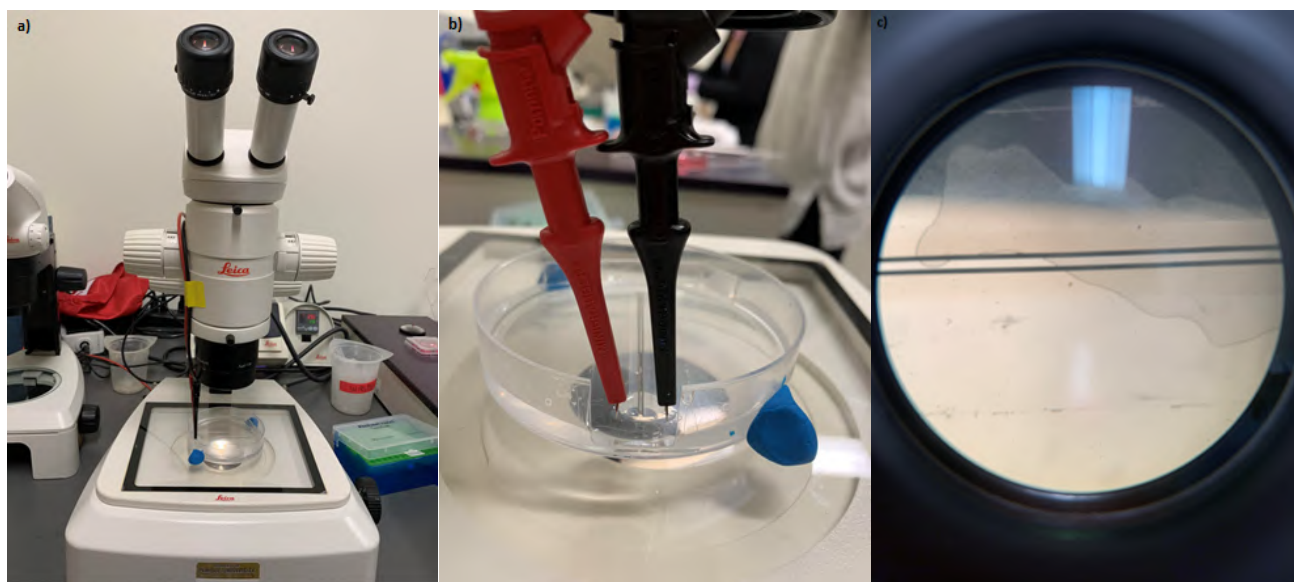
Figure 7a, b, c: Parthenogenetic activation system. a) Clay was used to hold the activation dish in place. b) Electrodes are attached to a pair of wires which electro-stimulate the oocytes causing parthenogenetic activation. c) Electrodes are fixed in the dish 1mm apart from each other. Oocytes are placed between the pair of electrodes for parthenogenetic activation.

2.5 In Vitro Culture (IVC)

In vitro fertilized zygotes were cultured in an incubator in a humidified atmosphere with 5% CO_2 in air at 39˚C. Parthenogenetically activated zygotes were cultured in a similar fashion, except in a hypoxic chamber with 5% O_2. 14-16 zygotes were cultured in 35 µL droplets of PZM3 (108 mM NaCl, 10 mM KCl, 0.35 mM KH_2PO_4, 0.40 mM $MgSO_4x7H_2O$, 25.07 mM $NaHCO_3$, 0.20 mM Na-pyruvate, 2.0 mM Ca-(lactate)$_2$x5H$_2$O, 1.0 mM L-glutamine, 5.0 mM hypotaurine, 20.0 mL/L BME, 10.0 mL/L MEM, 0.065 mg/mL penicillin, 0.050 mg/mL streptomycin), supplemented with 3 mg/mL bovine serum albumin (BSA). Under oil, 4-cell stage embryos were collected at 48 hours, and blastocyst stage embryos were collected 7 days post gamete mixing/parthenogenetic activation.

2.6 Nuclear Localization Sequence Mapping

Several nuclear localization signals (NLSs) were identified within the predicted amino acid sequences of BAF155 (XM_021068731) and BAF170 (XM_021092853) using an online NLS prediction platform (http://nls-mapper.iab.keio.ac.jp/cgi-bin/NLS_Mapper_form.cgi).

CHAPTER 3: TRANSCRIPT ABUNDANCE OF PORCINE BAF155 & BAF170

Rationale: The fluctuation of certain SWI/SNF subunit transcript abundance following different developmental stages indicates their importance to the developing embryo at each particular stage. In order to better understand the SWI/SNF scaffolding subunits, BAF155 and BAF170, in the developing embryo, it was necessary to examine their abundance at different stages of early development.

Hypothesis: Transcript abundance of *BAF155*/*BAF170* within the early porcine embryo will change in the course of early embryo development.

To test this hypothesis, first the sequence of transcripts for both porcine *BAF155* and *BAF170* was determined. Then, qPCR was performed to quantify transcript abundance in GV-stage oocytes, MII stage oocytes, 4-cell embryos, and blastocysts.

3.1 Sequencing of porcine *BAF155* & *BAF170* transcripts

Sequencing primer sets were tested using PCR to amplify a target transcript derived from cDNA isolated from porcine muscle or heart tissue mRNA. Porcine heart, muscle, and liver tissues were collected and flash frozen using liquid nitrogen before storage at -80˚ C until homogenization and mRNA processing using Dynabeads (See 3.2; Thermo Fisher, Waltham, MA, USA). The Thermo Scientific™ Revertaid™ First Strand cDNA Synthesis Kit was used for the synthesis of cDNA (Thermo Scientific, Waltham, MA, USA). Briefly, 1 µg of total mRNA was mixed with 1 µL of Random Hexamer primer. Water was then added to bring the total volume of the solution to 12 µL. The solution was then gently mixed, briefly centrifuged, and incubated at 65˚ C for 5

minutes. 4 µL of Reaction Buffer, 1 µL of RiboLock RNase Inhibitor, 2 µL of dNTP Mix, and 1 µL of RevertAid M-MulV RT were then added (in that order) to bring the total volume of solution to 20 µL. The solution was then mixed gently, briefly centrifuged, and incubated first at 25° C for 5 minutes, followed by 60 minutes at 42° C, and finally 70° C for 5 minutes for termination of the reaction. The cDNA was then stored at -20° C until use.

To amplify specific transcripts, 1 µL of cDNA was added to "sample" reactions. Their twin "non-template control" (NTC) reactions received 1 µL nuclease free water instead of cDNA. Each reaction utilized the same recipe: 0.4 µL of forward primer, 0.4 µL of reverse primer, 10 µL of Master Mix (ThermoFisher), and 9.2 µL of nuclease-free water. For primers, see Table 3. PCR program was as follows: 98° C for 10 seconds, 35 cycles of 98° C for 1 second, Tm of primer sets for 5 seconds (BAF155: 60° C; BAF170: 62° C), and 72° C for 1min/kb to be amplified, before reaction termination at 72° C for 10 minutes.

Gel electrophoresis (3g agar, 200mL 1x Tris base-acetic acid-EDTA (TAE), and 32µL ethidium bromide) was used to verify that the product was approximately the same size as the expected transcript length. Bands of the expected size were cut out of the agarose gel and purified according to Gel Purification kit instructions (QIAquick Gel Extraction Kit, QIAGEN, Hilden, Germany). Briefly, after the DNA fragment was excised from the gel, the gel fragment was weighed in a pre-weighed tube. Three volumes of Buffer QG were added to one volume of gel and incubated in a water bath at 50°C for ten minutes to dissolve the gel fragment. Then, one volume of isopropanol was added. The mixture was then placed in a spin column and centrifuged for 1 minute at 212 xg with the flow-through discarded post-centrifugation. Buffer QG (500 µL) was then added, and the tube was centrifuged at 212 xg for 1 minute. Next, Buffer PE (750 µL) was then added to wash the DNA and incubated for 5 minutes at room temperature. One minute

centrifugations at 212 xg were then performed twice, and the flow-through was discarded after each centrifugation. The column was then placed in a clean 2 mL collection tube. To elute the PCR fragments, 35 µL of Buffer EB were added to the center of the QIAquick membrane and left 1 minute at room temperature. Finally, the column was centrifuged for 1 minute at 212 xg, and DNA was collected.

A TOPO reaction was then performed to clone the PCR fragments into vectors according to TOPO kit instructions (pENTR/SD/D-TOPO, Invitrogen, Waltham, MA, USA). Briefly, 4 µL of the gel-purified PCR product was added to 1 µL of salt solution (1.2 M NaCl, 0.06 M $MgCl_2$) and 1 µL of TOPO vector and mixed gently. The mixture was incubated for 5 minutes at room temperature and then stored at -20˚C until use.

Table 3: Sequence Cloning Primers

Target	Forward Primer	Reverse Primer	Expected Product Size
BAF155	5'-CACCAGGATGCGCAGGCAG	5'-TACGAGCGTTGTCTAAAT	1070 bp
BAF170	5'- CACCATGGCGGTGCGGAAGAAG	5'- GAGAGATGTCTGGCTGGCTCC	1341 bp
M13	5'-GTAAAACGACGGCCAG	5'-CAGGAAACAGCTATGAC	-

Bacterial transformation of One Shot Top 10 chemically competent E. coli (Invitrogen, Waltham, MA, USA) was conducted with 3µL of TOPO reaction described above. The mixture was placed on ice for 30 min, then heat shock was applied for 45 seconds at 42˚C, followed by incubation on ice for another 2 minutes, and adding 250µL of SOC (2% tryptone, 0.5% yeast extract, 10 mM NaCl, 2.5 mM KCl, 10 mM MgCl2, 10 mM MgSO4, and 20 mM glucose) for

optimal transformation efficiency. Thereafter, the mixture was incubated for an hour at 37˚C while shaking and then plated on pre-warmed agarose plates containing kanamycin to selectively grow only insert-containing E. coli colonies. Two plates were prepared for each reaction, one using 50μL of bacterial mixture, the other using 100μL of bacterial mixture. Both plates were incubated overnight at 37˚C before being stored at 4˚C. Individual bacterial colonies were tested for the presence of target transcript. Patch plates were created to catalogue which individual colonies are tested. Patch plates were incubated at 37˚C overnight, then stored at 4˚C.

An M13 forward or reverse primer was substituted for either the subunit-specific forward or reverse primer (see Table 3) in order to excise the target transcript from the bacterial DNA. M13 primers anneal to a sequence contained within the bacteriophage vector. An M13 primer was used to ensure complete excision of the target sequence from the bacteriophage, as it is possible for nucleotides to be lost during transcript insertion into the vector. This loss of nucleotides would create difficulty for the annealing of the original forward or reverse primer. Gel electrophoresis was used to determine the size of the excised DNA segment.

Five mL of LB broth containing 25μL (10 mg/mL) kanamycin with a sample of an individual colony containing the correctly sized segment was incubated overnight at 37˚C while shaking to propagate E. coli cells containing the target sequence insert. A 250μL aliquot of the overnight culture was added to 250μL of sterile 50% glycerol and stored at -80˚C.

A Miniprep was then performed to extract the plasmid DNA using the remaining overnight culture according to kit instructions (PureLink Quick Plasmid Miniprep Kit, Invitrogen; QIAprep Spin Miniprep Kit, QIAGEN). Briefly, the overnight culture was centrifuged for 10 minutes at 12000 xg and the supernatant was removed from the pellet. This pellet was resuspended in 250

µL of Resuspension Buffer (R3) with RNase. The suspension was lysed by adding 250 µL of Lysis Buffer (L7) and mixed gently by inverting the capped tube, followed by incubation for 5 minutes at room temperature. To precipitate chromosomal DNA, cellular debris, and denatured protein, 350 µL of Precipitation Buffer (N3) was added to the suspension, and the tube was inverted repeatedly. Another 10 minute centrifugation at 12000 xg was performed. The supernatant containing plasmid DNA was loaded onto a spin column provided by the kit, then centrifuged at 12000 xg for 1 minute. The flow-through was discarded, and the spin column containing plasmid DNA was replaced and washed with 500 µL of Wash Buffer (W10) for 1 minute at room temperature, then centrifuged at 12000 xg for 1 minute. The flow-through was then discarded. 700 µL of Wash Buffer (W9) with ethanol (30 mL ethanol added to 12 mL W9) was then added to the column. Two subsequent centrifugations at 12000 xg for 1 minute were performed without additional washings, with the flow-through being discarded between centrifugations. The spin tube was then transferred to a 1.5 mL recovery tube provided by the kit. Seventy-five µL of preheated TE buffer (70°C) was added to the center of the spin column and incubated for 1 minute at room temperature, followed by centrifugation at 12000 xg for 2 minutes and storage of eluted plasmid DNA at -20°C until use. This Miniprep was sequenced at the Low Throughput Lab (Purdue University). Purdue's Low Throughput Lab runs samples on an ABI 3730XL using BigDye v3.1 Cycle Sequencing terminator chemistry. Samples are run twice if less than 600 High Quality Bases are acquired for a particular sample. One µL of sample is utilized to determine the concentration of template.

3.1.1 Results

The transcript sequences of the target subunits of this study, *BAF155* and *BAF170*, had not yet been sequenced from porcine tissue. Primer sets were designed to accomplish this task (See Table 3), utilizing both muscle and heart tissues as source of mRNA.

The Purdue Low Throughput Lab raw sequencing results for *BAF155* transcript are as follows (903 bp):

```
GATATACTTGGCATATAGAAATTTTATGATCGACACATATCGCCTAAATCCCCAAGA
ATATTTAACTAGCACTGCCTGTCGGAGGAACTTGACTGGAGATGTGTGTGCTGTGAT
GAGAGTTCATGCCTTTTTAGAGCAGTGGGGGCTTGTTAATTACCAAGTGGATCCAGA
AAGTCGACCGATGGCAATGGGACCTCCTCCAACCCCTCATTTCAATGTCTTAGCTGA
CACTCCCTCTGGGCTGGTGCCTCTACATCTTCGATCACCTCAGGTTCCTGCTGCTCAG
CAGATGTTAAATTTTCCTGAGAAGAACAAGGAAAAACCAATTGATTTGCAGAACTTT
GGTCTTCGTACTGACATTTATTCCAAGAAAACATTAGCAAAGAGCAAAGGTGCTAGT
GCTGGAAGAGAATGGACTGAACAGGAGACCCTTCTACTTCTTGAGGCCCTAGAGAT
GTATAAGGATGATTGGAACAAAGTGTCAGAACATGTTGGAAGTCGCACGCAAGATG
AATGCATCCTCTACTTTTTGAGGCTTCCCATTGAGGACCCATACCTTGAGAATTCAG
ATGCTTCTCTAGGGCCCCTGGCCTACCAGCCTGTCCCCTTCAGTCAGTCGGGAAACC
CAGTCATGAGCACTGTTGCTTTTTGGCGTCTGTGGTAAGGGGTGGGCGCGCCGACC
CAGCTTTCTTGTACAAAGTTGGCATTATAAGAAAGCATTGCTTATCAATTTGTTGCA
ACGAACAGGTCACTATCAGTCAAAATAAAATCATTATTTGCCATCCAGCTGATATCC
CCTATAGTGAGTCGTATTACATGGTCATAGCTGTTTCCTGGCAGCTCTGGCCCGTGTC
TCAAAATCTCTGATGTTACATTGCACAAGATAAAAATATATCATCATG
```

The Purdue Low Throughput Lab raw sequencing results for *BAF170* transcript are as follows (1341 bp):

```
CCATTCAGAGCAGTACTACGAGGCGCGGACACCGTGACCCAGTTCGACAACGTGCG
GCTCTGGCTTGGCAAGAACTACAAGAAGTATATACAAGCTGAACCACCTACCAACA
AGTCCCTGTCTAGCCTGGTTGTACAATTGCTACAATTTCAGGAAGAAGTTTTTGGCA
AACATGTCAGCAATGCACCTCTCACTAAACTGCCGATCAAATGTTTCCTAGATTTCA
AAGCAGGAGGCTCCCTGTGCCACATACTTGCAGCTGCCTACAAATTCAAGAGTGAC
CAGGGATGGCGGCGTTACGATTTCCAGAATCCATCACGCATGGACCGCAATGTGGA
AATGTTCATGACCATTGAGAAGTCCTTGGTGCAGAATAATTGCCTGTCTCGACCTAA
CATTTTTCTGTGCCCAGAAATTGAACCCAAACTGTTAGGGAAATTAAAGGACATTAT
CAAGAGACATCAGGGGACGGTCACTGAGGAGAAGAACAATGCCTCCCATGTTGTGT
GTCCTGTCCCAGGGAACCTGGAGGAAGAGGAATGGGTACGGCCAGTCATGAAGAGG
GATAAGCAGGTTCTTCTGCACTGGGGCTACTATCCTGACAGTTACGACACATGGATC
CCAGCCAGTGAAATTGAAGCATCTGTGGAAGATGCTCCAACTCCTGAGAAACCCAG
```

AAAGGTTCACGCAAAGTGGATCCTGGACACAGACACCTTCAATGAATGGATGAATG
AGGAAGACTATGAAGTGAATGATGACAAAAACCCTGTCTCGCGCCGAAAGAAGATA
TCAGCCAAGACATTGACAGACGAGGTGAACAGCCCAGATTCAGATCGACGGGACAA
GAAAGGAGGGAACTATAAGAAGCGGAAACGCTCCCCCTCTCCTTCACCGACCCCAG
AAGCTAAGAAGAAGAATGCCAAGAAAGGTCCCTCAACACCTTACACCAAGTCAAAG
CGTGGCCACAGAGAAGAGGAGCAAGAAGACCTGACAAAGGACATGGAATGAGCCC
CTCACCGGGTTCCCAATGTGAAGAGTGACGTTGCCCCAAAACAGTCAACACTAAAG
AAGGACTTCAGAGTCAGCCCCGGGTCAAGGAGGCACCATGACGGGACCCTGGGAT
GAACAAGAAGATGAGAGCATGCAGACTACGGCCAGAATGAAGATGAGAACAGTAC
GGGAACCAGGGGAGAGCAGACCCAAGAAATCCGGAACCTACACGAGGACAATGTG
ACCGGAACAAGAGCCACCACATCATCATTCCCAAGCCTACGCTGCTGGATGGACCT
ATAAAAATGTTCCATGCCATAAGAGCGGAGGCCTCTCTCC TCGGAGATATA

When the transcript sequences were compared to known sequences using NCBI's Blast tool (National Institutes of Health, Stapleton, NY, USA), homology to human and mouse *SMARCC1* (*BAF155*) and *SMARCC2* (*BAF170*) was high. In the case of *SMARCC1* (*BAF155*), homology to human *BAF155* was 92.45%, homology to mouse *Baf155* was 89.98%. The full predicted length for Sus scrofa *BAF155* is 5658 base pairs; with the successfully sequenced portion of the transcript covering 15.96% of the predicted sequence length. The successfully sequenced portion of transcript begins 1473 base pairs from the 5´ end of the predicted *Sus Scrofa BAF155* sequence (XM_021068731). In the case of *SMARCC2* (*BAF170*), homology to human *BAF170* was 92.13%, homology to mouse *Baf170* was 88.01%. The full predicted length for *Sus scrofa BAF170* is 4714 base pairs, with the successfully sequenced portion of the transcript covering 28.45% of the predicted sequence length. The successfully sequenced portion of transcript begins 147 base pairs from the 5´ end of the predicted *Sus Scrofa* BAF170 sequence (XM_021092853).

3.2 Transcript Abundance of *BAF155/BAF170* Determined by qPCR

mRNA was isolated from pools of 100-800 denuded GV stage oocytes frozen at -80°C in 100µL of Dynabeads' lysis buffer according to the manufacturer's instructions (Thermo Fisher).

Prewashed Dynabeads were incubated with 100 µL of lysed embryos/oocytes and rotated at room temperature for 5 minutes. The magnet strip was then used to pull down the beads/RNA, and the supernatant was removed. Then, two washes with 100 µL of Buffer A were performed and the supernatant was removed between washes. 100 µL of Buffer B was added to the Dynabeads/RNA and transferred to a tube on ice. The supernatant was removed followed by another wash with 100 µL of Buffer B. Beads/RNA were then resuspended in 100 µL of Tris-HCL and the supernatant was removed. Thirty µL of cold RNase-free water was added to the beads and the bead/water slush was transferred to two PCR tubes (15 µL each). One µL of reverse transcriptase was added to the RT+ tube. Water was added in place of reverse transcriptase in order to create a negative control for each cDNA reaction (RT-). Water was added to obtain a total volume of 20 µL in each tube. Each mRNA sample was reverse transcribed to cDNA, and *BAF155* or *BAF170*, and *YHWAG* (housekeeping gene) were amplified using reverse transcription-polymerase chain reaction (Wang et al. 2012). Non-template controls (no mRNA, NTCs) and reverse transcriptase negative (RT-) samples were run in parallel with reverse transcriptase positive (RT+) samples to confirm lack of DNA contamination. A CFX Connect Real-Time System for PCR detection (Bio-Rad) was used for all RT-PCR reactions. Each PCR reaction contained 10 µL of SybrGreen Mastermix (Bio-Rad), 2.8 µL of 10 µM forward primer, 2.8 µL of 10 µM reverse primer, 8.4 or 11.4 µL of nuclease-free water, and 3 or 6 µL cDNA. cDNA concentration is increased for low template cDNA. Nuclease-free water was utilized to bring the total volume of each reaction to 30 µL. For primer sequences, see Table 4. Each reaction was performed in duplicate. The PCR program was comprised of an initial denaturation at 94°C for 5 min, followed by 40 cycles of 5 s at 94°C, 30 s at 60°C, and 30 s at 72°C. Real-time fluorescence data were collected during the extension time after each cycle.

BAF155 or *BAF170,* and *YWHAG* were amplified in parallel; the threshold cycle of detection (or CT value) for *BAF155* or *BAF170* was documented. *YWHAG* CT values were also collected and compared to known transcript abundance of *YWHAG* to verify the quality of the oocytes or embryos and that reactions were performed correctly. *YWHAG* is known as a "housekeeping gene", meaning that it is present in all cells of an organism and required for the basic maintenance of cellular function. Importantly, it has been shown not to change in transcript abundance during early embryonic development. This allows for it to be used to compare relative abundance changes of other transcripts at different developmental stages. A melt curve was analyzed to verify singular PCR products.

Table 4: RT-PCR primers

Targeted Subunit	Forward Primer	Reverse Primer
BAF155	A: 5'-GAGGAACTTGACTGGAGATGTG	A: 5'-ATTGCCATCGGTCGACTTT
BAF170	C: 5'-AGAGTCGACCAACCCCAATG	C: 5'-GTCTGCTGCGGGGTCTTG
YHWAG	5'- TCCATCACTGAGGAAAACTGCTAA	5'- TTTTTCCAACTCCGTGTTTCTCTA

Minipreps generated in 3.1 served as templates for standard curves do determine primer efficiency ranges. Primer sets (See Table 4) targeting fragments of each sequence (100-200bp) were utilized to obtain Standard Curves for different dilutions of template to determine CT-values which correspond to known amounts of progressively diluted template. One-in-ten serial dilutions were performed to create the standard curves. Dilutions were made using nuclease-free water.

3.2.1 Results

Ideally, the number of molecules during each replication cycle doubles, corresponding to an amplification efficiency of 100%. Similarly, amplification factor would ideally be 2.0, corresponding to a doubling of molecules each replication cycle. The CT-range is the range at which the primer set is efficiently amplifying the target transcript. CT readings must be within the CT-range to allow accurate quantification of transcript in a sample. Outside of the determined CT-range, the primers are not efficiently amplifying the target sequence at a rate of double/cycle.
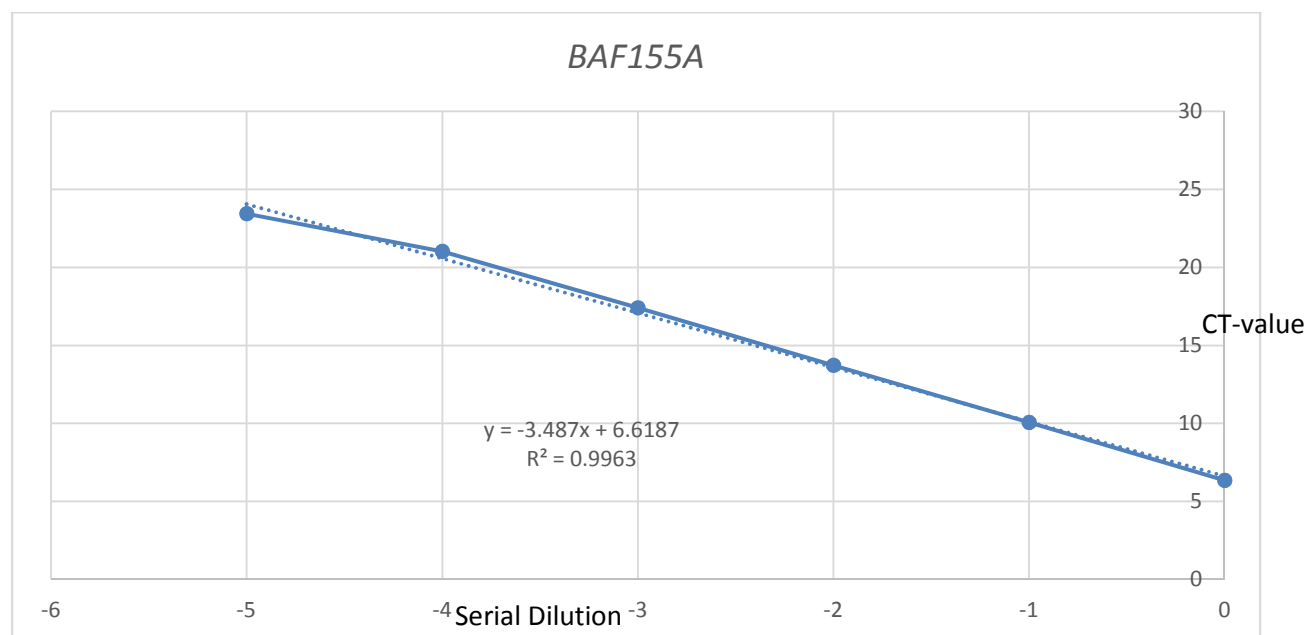
Amplification efficiency: 93.54%; Amplification factor: 1.94; CT-range: 6.35 - 23.44

Figure 8: Standard curve for *BAF155*
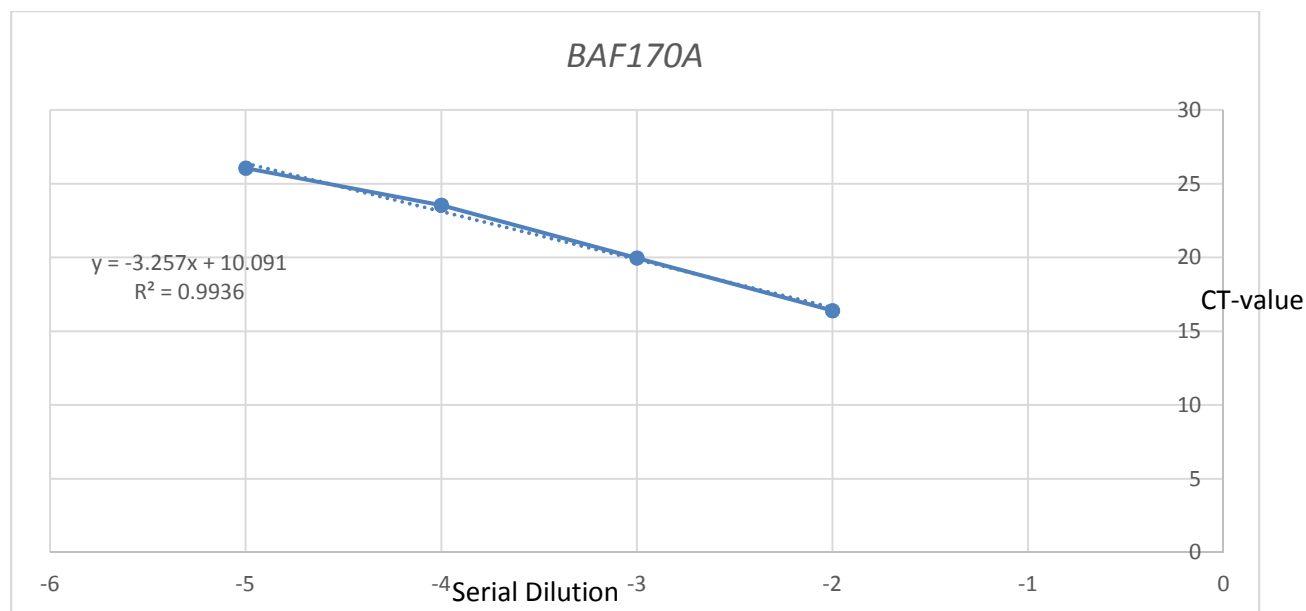
Amplification efficiency: 102.78%; Amplification factor: 2.03; CT-range: 16.39 – 26.06

Figure 9: Standard curve for *BAF170*

Preliminary real time polymerase chain reactions (RT-PCR) were performed to determine a standard for transcript levels of oocytes. The standard curve for *YWHAG* was previously determined, with expression remaining constant throughout cleavage development (Magnani and Cabot, 2007; Whitworth et al. 2005).

Pools of 100-600 GV or M2 stage oocytes were lysed, mRNA was converted into cDNA, and analyzed as described above. However, transcript abundance was too low for reliable quantification of both *BAF155* and *BAF170* (CT values $\geq$ 27.33; CT-range for reliable assessment of *BAF155*: 6.35-23.44, CT-range for reliable assessment of *BAF170*: 16.39–26.06). qPCR was also performed for *BAF155* on a pool of cDNA derived from 52 blastocysts. Again, transcript abundance of *BAF155* was too low for a reliable prediction of transcript levels (CT=35.25; see Table 5).

Table 5: Average CT values from duplicates of *BAF155* transcript abundance in pools of GV and M2 oocytes as well as blastocyst stage embryos. Pool sizes are reflected in the top row.

Subunit/Input	100 GV	220 GV	300 GV	600 GV	600 M2	52 Blast
BAF155	28.01	27.33	29.83	29.51	31.35	35.25
YWHAG	27.00	23.63	23.08	22.40	22.97	32.77

Table 6: Average CT values from duplicates of *BAF170* transcript abundance in pools of GV and M2 oocytes. Pool sizes are reflected in the top row.

Subunit/Input	132 GV	300 GV	600 GV	600 M2
BAF170	31.3	29.50	29.50	29.96
YWHAG	25.11	22.98	23.66	22.39

Transcript abundance of both *BAF155* and *BAF170* was too low to be accurately quantified using our current primer sets despite the drastic increase in input.

3.3 Discussion

Transcript abundance changes of different subunits have been shown to fluctuate dynamically during different stages of porcine embryo development. In the porcine model, *SMARCA4* (*BRG1*), a SWI/SNF ATPase, abundance is first downregulated in the MII oocyte in relation to transcript levels seen in the GV oocyte. Transcript level then becomes similar to the GV oocyte in the 2-cell, 4-cell, 8-cell, and blastocyst stages (Magnani and Cabot, 2009). In the rhesus monkey, transcript abundance of *BRG1* declines similarly to the pig during oocyte maturation.

The *BRG1* transcript is present as maternal mRNA until the morula stage, which is the time of zygotic genome activation (Zheng et al. 2004). The other SWI/SNF ATPase, *SMARCA2* (*BRM*), also shows transcript levels are downregulated at the MII stage in comparison to GV oocytes. However, transcript abundance of *SMARCA2* continues to decrease, reaching its' lowest in the 8-cell and blastocyst stages (Magnani and Cabot, 2009). In the rhesus monkey embryo, the transcript of *BRM* is present as maternal mRNA until the hatched blastocyst stage (Zheng et al. 2004). *ARID1A* shows significantly reduced transcript levels at the 4-cell stage compared to GV oocytes, indicating that *ARID1A* is important to cleavage-development. This is proven when the *ARID1A* knockdown significantly reduced nuclei numbers after seven days of *in vitro* culture (Tseng et al. 2017). Understanding the transcript abundance of the scaffolding subunits, *BAF155* and *BAF170*, is important to realizing their significance during specific developmental events in the porcine embryo.

The protocol used reduces the number of oocytes or embryos present within each qPCR reaction. For example; if 600 GV oocytes are lysed, those oocytes will be halved to create the RT+ and RT- reaction tubes. Out of the 20 µL reaction tube, only 3 or 6 µL are utilized per reaction (dependent upon template concentration). This brings the 300 oocytes per reaction tube to either 45 oocytes (for 3 µL) or 90 oocytes (for 6 µL) per qPCR reaction. Thus, although the amount of oocytes first lysed is large, the oocytes actually analyzed are much smaller.

The process of collecting enough oocytes and blastocyst stage embryos to analyze *BAF155* and *BAF170* transcript abundance with the technology used here was unsuccessful because resources are limited. A possible solution for this experiment would be to design and test a variety of different primer sets with the goal to obtain higher CT values, thus allowing for lower transcript abundances to be accurately quantified.

There are several reasons why we might see an increase or a lack of change in CT-value despite an increase in the amount of pooled GV oocytes (see Table 5 & 6). First of these is the inconsistency of quality of oocytes. Because we have no control over the age, pubertal maturation, or health of the pigs from which our ovaries are collected, we cannot control the quality of the oocytes aspirated from those ovaries. Transcript abundance of *BAF155* and/or *BAF170* conceivably fluctuate with the maturation of oocytes, so the percentage of those GV oocytes closer to ovulation at the time of aspiration (and thus more mature) will cause the CT-values to fluctuate from what is expected.

The production of too much or too little cDNA during cDNA synthesis can also alter the CT-values in unexpected ways (ThermoFisher). Ratios of cDNA to primers need to be optimal for the most accurate readings by the qPCR machine. However, to avoid introduction of another variable, the working stock of the reactions was not changed between experiments. Similarly, the cDNA concentration was not checked after production. In future experiments, changing the recipe of the reactions' working stock in order to optimize primer to cDNA ratio can increase efficiency and help lessen the variation seen in CT-values.

CHAPTER 4: DEVELOPMENTAL REQUIREMENTS OF BAF155 & BAF170

Rationale: Chromatin remodeling complexes, such as the SWI/SNF complexes, are important to the development of the embryo. Scaffolding subunits of the SWI/SNF complex, BAF155 and BAF170, are necessary to maintain the integrity of the complex as a whole. Study of the effects of the depletion of BAF155, BAF170, or both simultaneously was necessary to understand the importance of one, or both, subunit(s) to the developing embryo. Observation of stage of arrest, or the absence of arrest, provides indications concerning the different requirements of one or both of these subunit(s). The outcome of this experiment will provide insight into the potential for compensation of one or both subunits following the loss of its heterodimeric partner, through formation of a functional homodimer.

Hypothesis: Reduced transcript abundance of *BAF155*, *BAF170*, or *BAF155* and *BAF170* in combination will reduce the developmental competency of the early porcine embryo.

To test this hypothesis, an efficient manner of measuring the developmental competency as well as knocking down target transcripts was necessary. An interfering RNA assay was designed to first test embryonic developmental competency post-knockdown of *BAF155*, *BAF170*, and finally both transcripts combined. Average nuclei numbers of treatment and control groups were evaluated using SAS (SAS Institute Inc, Cary, NC, USA) ANOVA with significant differences between treatment and control group nuclei averages (Tukey) indicative of changes in developmental competency. *In vitro* fertilized embryos and parthenogenetically activated embryos were evaluated separately. A p-value of <0.05 was considered significant.

4.1 RNA interference assay

Naturally occurring double stranded RNAs (dsRNA) are produced in the embryo in order to knockdown the translation of target messenger RNA (mRNA) into proteins. These dsRNAs are cleaved into small fragments before binding to Argonaute proteins which separate the dsRNA into single stranded RNA. Now termed small interfering RNA (siRNA), the fragment is incorporated into the RNA-induced silencing complex (RISC). siRNA may also be introduced via microinjection in order to achieve similar knockdown effects. The RNA fragments are then cleaved before binding to their complementary sequences located on target mRNAs. The Argonaute proteins are then able to degrade the bound mRNA, thus knocking down the target transcript.

An Eppendorf Femtojet injector was used during all oocyte and embryo microinjection assays (Eppendorf, Hauppauge, NY, USA). The Femtojet was attached to a Leica DMi 8 inverted microscope system which was equipped with a heating stage (Leica, Bufallo Grove, IL, USA). The holding pipette was attached to an Eppendorf CellTram Air micromanipulator (Eppendorf, Hamburg, Germany). Presumed zygotes 5 hours post gamete mixing or parthenotes immediately following activation were placed in TL-HEPES medium containing 3 mg/mL bovine serum albumin for micromanipulation. Individual embryos were held with a holding pipette while small interfering RNAs (1 nM) were injected with an injection pipette. Care was taken to ensure that the injection pipette penetrated not only the zona pellucida, but also the elastic plasma membrane. Correct delivery of the construct into the cytoplasm was validated by the observation of gentle movement of lipid droplets in the cytoplasm during injection. Embryos with an intact plasma membrane were cultured as described in the Materials and Methods.

BAF155 and BAF170: To study the effects of a *BAF155* or *BAF170* knockdown, presumed zygotes/parthenotes were microinjected with small interfering RNA (siRNA) targeting BAF155 or BAF170 five hours post gamete mixing or immediately after activation. Three treatments were performed:

1) Injection with siRNA targeting BAF155, BAF170, or both (mixed together 1:1)

2) Injection with Scramble-RNA for BAF155, BAF170, or both (mixed together 1:1)

3) Not injected.

siRNA was designed using the Invitrogen stealth RNA design tool and ordered through Thermo Fisher. Each stealth RNA included a paired scramble RNA for use as a control.

Table 7: BAF155 and BAF170 siRNA, and Scramble-RNA

Targeted	siRNA (antisense)	Scramble-RNA (antisense)
BAF155	AUUACGAUCCAUUCGGGAUGGAUUC "stealth_73"	AUUGAACGAUCCAUUCGGGAUGUUC "stealth_control_73"
BAF170	UGUCUUGGCUGAUAUCUUCUUUCGG "XM_003481619.3_stealth_939"	UGUUUCGGUUAGUCCUAUUCUUCGG "XM_003481619.3_stealth_control_939"

Embryos were cultured in PZM3 in their respective treatment groups at 39°C in 5% CO_2 (see 2.5). Embryos were collected 7 days after *in vitro* fertilization or parthenogenetic activation. Embryos were fixed 7 days post-fertilization/activation in 3.7% paraformaldehyde at 4°C for 1 hour, washed three times (30min/wash) in phosphate-buffered saline with 0.1% Tween20 (PBS-T), and stored in PBS-T, at 4°C until further processing (up to 14 days). Fixed embryos were then permeabelized using PBS/1% Triton X-100 medium for 1 hour at 4 °C and washed once

(30min) in PBS-T followed by a 15min incubation in Hoechst Solution 33324 (2µg/mL; BDbioscience cat: 561908). Embryos were mounted on slides in Vectashield (Vector Laboratories, Burlingame, CA, USA), covered with a glass coverslip and sealed with nail polish. Embryos were examined using a Leica DMi 8 inverted microscope equipped with epifluorescence as well as a Nikon A1R-MP confocal microscope (Leica, Wetzlar, Germany; Nikon, Chiyoda, Japan). Hoechst was viewed at a wavelength of 405 nm. Embryos were assessed with individual nuclei numbers recorded for each individual embryo.

4.1.1 Results

Table 8: Developmental competency of BAF155 siRNA injected porcine embryos

BAF155	Average Cell #	Average Cell # (≥ 2 cells)	Morphological Blastocyst %	Morphological Blastocyst % (≥ 2 cells)
Non-Injected	5.04[a]	8.95[a]	8.63[a] (27/313)	17.09[a] (27/158)
Scramble RNA	4.35[a]	7.72[a]	6.71[a] (23/343)	13.14[a] (23/175)
siRNA	5.56[a]	8.89[a]	9.78[a] (31/317)	17.61[a] (31/176)

Individual embryo's nuclei numbers were evaluated after 7 days of *in vitro* culture and an analysis of variance (ANOVA) was performed. Two sets of averages were used: (1) including all embryos (2) including only embryos which had cleaved at least once. Significant differences between means are shown at $P<0.05$.

No significant difference between Non-Injected, Scramble RNA, and *BAF155* siRNA groups was seen in this study. This indicates that the knockdown of *BAF155* does not cause significant developmental detriment to the preimplantation porcine embryo. Three replicates of *in vitro* fertilized embryos were evaluated.

Table 9: Developmental competency of BAF170 siRNA injected porcine embryos

BAF170	Embryo Source	Average Cell #	Average Cell # (≥ 2 cells)	Morphological Blastocyst %	Morphological Blastocyst % (≥ 2 cells)
Non-Injected	IVF	1.57^a	3.41^a	8.16* (4/49)	23.53* (4/17)
	PA	4.80^d	6.37^d	6.17^d (14/228)	11.67^d (14/120)
Scramble RNA	IVF	2.12^a	3.44^a	1.52* (1/65)	3.13* (1/32)
	PA	2.80^e	4.80^{de}	4.29^{de} (7/163)	8.05^d (7/87)
siRNA	IVF	2.04^a	2.9^a	0* (0/66)	0* (0/41)
	PA	2.23^e	3.12^e	0^e (0/102)	0^e (0/39)

Individual embryo's nuclei numbers were evaluated after 7 days of *in vitro* culture following IVF/PA and an analysis of variance (ANOVA) were performed. Two sets of averages were used: (1) including all embryos (2) including only embryos which had cleaved at least once. Significant differences between means (P<0.05) are indicated by superscripts. * is used to denote groups with too few replicates to be statistically specified.

Similarly, there was no significant difference observed between Non-Injected, Scramble, and *BAF170* siRNA groups with the exception of those derived using parthenogenetic activation. With the consideration of all activated embryos, there were significant differences between Non-Injected and Scramble groups as well as Non-Injected and siRNA groups. Parthenogenetically activated embryos which had reached cleavage stage presented a significant difference exclusively between Non-Injected and siRNA groups. However, those embryos produced via *in vitro* fertilization did not show any significant difference between the Non-Injected, Scramble, or siRNA groups. A single replicate of IVF-derived embryos was evaluated alongside three replicates of parthenogenetically activated embryos. Morphological blastocysts maintained the same statistical results as their average nuclei number counterparts with the exception of the >2 nuclei group, whose siRNA group was significantly different from both the Non-Injected and Scramble groups. No statistical analysis was performed, because only one replicate was done for

IVF embryos. Parthenogenetic embryos were added after *in vitro* fertilization protocols failed to create blastocyst stage embryos in Non-Injected groups multiple weeks in a row.

Table 10: Developmental competency of combined BAF155/BAF170 siRNA injected embryos

BAF155/BAF170	Oocyte Activation	Average Cell #	Average Cell # (≥ 2 cells)	Morphological Blastocyst %	Morphological Blastocyst % (≥ 2 cells)
Non-Injected	IVF	1.37[a]	3.17[a]	4.51[a] (6/133)	13.95[a] (6/43)
	PA	3.91[d]	5.63[d]	7.86[d] (11/140)	11.96[d] (11/92)
Scramble RNA	IVF	2.77[ab]	4.90[a]	4.88[a] (6/123)	9.68[a] (6/62)
	PA	4.38[d]	6.32[d]	6.25[e] (5/80)	9.43[d] (5/53)
siRNA	IVF	2.76[b]	4.37[a]	2.42[a] (3/124)	4.41[a] (3/68)
	PA	3.63[d]	5.04[d]	2.94[f] (2/68)	4.26[d] (2/47)

Individual embryo's nuclei numbers were evaluated after 7 days of *in vitro* culture following IVF/PA and an analysis of variance (ANOVA) was performed. Two sets of averages were used: (1) including all embryos (2) including only embryos which had cleaved at least once. Significant differences between means ($P<0.05$) are indicated by superscripts.

Further, when considering the simultaneous injection of both BAF155/BAF170 siRNA there was no significant difference between Non-Injected, Scramble, and siRNA treatment groups in parthenogenetically activated embryos. Considering all in vitro embryos, there was a significant difference between Non-Injected and siRNA groups. For those in vitro embryos which had reached cleavage stage (>2 cells) significant differences were seen between Non-Injected and Scramble groups as well as Non-Injected and siRNA groups. Two replicates of *in vitro* fertilized embryos and two replicates of parthenogenetically activated embryos were evaluated. When considering morphological blastocyst percentages, the only group which showed significant difference was the parthenogenetically activated embryos. This group showed statistical difference only between the Non-Injected and siRNA groups. Parthenogenetic embryos were

added after *in vitro* fertilization protocols failed to create blastocyst stage embryos in Non-Injected groups multiple weeks in a row.

4.2 Discussion

Baf155 and Baf170 have been shown to be crucial to murine embryonic development. Mutations in *Baf155* transcript creates disorders in neural tube development, resulting in the absence of a major portion of the brain and scalp (anencephaly) or the development of the brain outside of the skull (exencephaly) (Harmacek et al. 2014). While a knockout of murine *BAF170* does not lead to the same level of catastrophy, embryonic knockouts are resultant in an increase in neural tube thickness (Tuoc et al. 2013). In humans, loss or mutation of *BAF170* has been implicated in neural disorders such as Coffin-Siris syndrome (Machol et al. 2018).

The only groups which showed a significant difference between control and siRNA treatment groups without a difference between Non-Injected and Scramble controls was the cleavage stage *BAF170* siRNA embryos created via parthenogenetic activation, morphological blastocysts of *BAF170* siRNA created via parthenogenetic activation, and morphological blastocysts of *BAF155/BAF170* siRNA created via parthenogenetic activation. All other groups showed either (1) no significant difference between treatment and control groups or (2) significant differences between Non-Injected and Scramble controls alongside the siRNA treatment group. Significant differences between Non-Injected and Scramble groups are only seen in groups including all embryos, suggesting that the difference is due to the death of embryos post-selection for *in vitro* culture. The results indicate that the knockdown of *BAF155*, *BAF170* (only one replicate performed), and *BAF155/BAF170* combined does not have a significant impact on embryonic development.

Parthenotes were used for both BAF170 and BAF155/BAF170 experiments due to problems involving the semen quality. Parthenogenetic activation is an alternative to studying preimplantation embryos. Parthenogenetically activated porcine embryos are able to develop to E30 post-activation (Zhu et al. 2003). However, development is terminated due to lack of imprinted paternal genes which are required to establish a functional placenta. Parthenotes resorb a polar body to replace the genetic component typically provided by the spermatozoa (Bos-Mikich et al. 2015). Because our work is focused on embryonic Day 1-7, parthenogenetic embryos are an efficient alternative to *in vitro* produced embryos.

The murine and porcine embryogenesis timelines must be considered when evaluating the results in this study. Murine embryos develop at an exceedingly faster pace than porcine embryos, reaching blastocyst stage at E3. By contrast, porcine embryos reach blastocyst stage at E6-7. In the investigative studies previously mentioned, mutant BAF155 murine embryos were evaluated at E9.5, while BAF170 conditional KO murine embryos were evaluated at the earliest on E10.5, both studies occurring alongside development of the neural crest (Harmacek et al. 2014; Tuoc et al. 2013). Considering the gestational length of mice is 18-22 days while pig gestation is 114 days, the maturity at which an E9.5-10.5 murine embryo and an E7 porcine embryo are vastly different. This suggests that the knockdown of *BAF155* and/or *BAF170* may exhibit a development effect in porcine embryos, however it is not recognizable until later in development.

Interestingly, BAF155 has been shown to bind and protect SNF5, another SWI/SNF core subunit, from proteasomal degradation (Jung et al. 2012). As previously speculated, it is highly likely that the binding of BAF155 to BAF170 in heterodimer formation also protects BAF170 from proteasomal degradation, although this was not explored in study. This binding and

protection of proteins by BAF155 results in an increase in protein half-life. Therefore, despite knockdown of *BAF155* and *BAF170* transcript, the presence of maternal BAF155/BAF170/SNF5 core proteins might maintain the integrity of SWI/SNF complexes at least until the blastocyst stage in porcine embryos.

CHAPTER 5: BAF155 & BAF170 NUCLEAR IMPORT BY KARYOPHERIN ALPHA 7

Rationale: It has been shown in the porcine embryo model that individual subunits, e.g. BRD7, of the SWI/SNF complex are imported by karyopherin alpha 7 (KPNA7) from the cytoplasm to the nucleoplasm. The specific transporters of BAF155 and BAF170 in the porcine embryo are unknown; however, because KPNA7 actively imports other subunits of the SWI/SNF complex, it is conceivable KPNA7 also imports BAF155 and/or BAF170.

Hypothesis: KPNA7 acts as the main transporter of BAF155 and/or BAF170. Therefore, depletion of competent KPNA7 will affect localization patterns for BAF155 and/or BAF170 proteins.

To test this hypothesis, a way of sufficiently decreasing active KPNA7 was implemented. We utilized two separate methods. The first was microinjection of a dominant-negative (DN) *KPNA7*; which was able to bind to the cargo, but unable to bind to karyopherin beta (KPNB), preventing it from being transmitted through the nuclear pore complex and into the nucleoplasm. The second was an injection of siRNA targeting *KPNA7*, decreasing the amount of *KPNA7* transcript. The embryos were injected post parthenogenetic activation and cultured for 48 hours. Four-cell embryos were collected and analyzed immunocytochemically to determine BAF155 and BAF170 localization patterns.

5.1 Inhibiting nuclear import via KPNA7

5.1.1 DN-KPNA7 Design

We hypothesized that KPNA7 is a main transporter of BAF155 and/or BAF170, and therefore that the introduction of a DN-KPNA7 construct affects the movement of BAF155/BAF170 from

the cytoplasm into the nucleoplasm. A dominant-negative KPNA7 mRNA construct tagged with green fluorescent protein (GFP) was previously designed lacking the importin β binding (IBB) domain (Crodian et al. 2019). This missing domain still allows the KPNA7 to bind to the cargo, but not to KPNB. Without the binding of KPNB, the dimeric complex cannot bind to nuclear pore complex and move from the cytoplasm through the nuclear envelope and into the nucleoplasm. Overexpression of the DN-KPNA7 will outcompete with the competent wild-type KPNA7 protein. The GFP tag allows determination of the intracellular localization of the translated DN-KPNA7 construct. This tag therefore serves as control, confirming successful injection and translation of the construct within the embryo.

5.1.2 RNA interference assay

To further study the effects of a *KPNA7* knockdown, oocytes were microinjected with small interfering RNA (siRNA) targeting *KPNA7* immediately following parthenogenetic activation. The *KPNA7* siRNA was validated in-lab previously (Wang et al. 2012).

Three treatments were performed similar to those described in Chapter 4.

1) Injection with siRNA targeting *KPNA7* (1nM),

2) Injection with Scramble-RNA for *KPNA7* (1nM)

3) Not injected.

Microinjection was performed equivalent to the previously described procedure (see 4.1). Embryos of treatments 1,2 & 3 were evaluated at 48 hours post-activation (4-cell) and Day 7 post-activation for treatment 3, which serves as a control for embryo quality and developmental competency.

5.1.3 Immunocytochemistry

For studying KPNA7-mediated import of BAF155 or BAF170 by immunocytochemistry, embryos were fixed 48 hours post-activation in 3.7% paraformaldehyde at 4°C for 1 hour, washed three times (30min/wash) in phosphate-buffered saline with 0.1% Tween20 (PBS-T), and stored in PBS-T at 4°C until further processing (up to 14 days). Fixed embryos were then permeabelized using PBS/1% Triton X-100 medium for 1 hour at 4 °C and washed once (30min) in PBS-T. Blocking was performed for 18 hours using blocking solution (0.1 M glycine, 1% goat serum, 0.01% Triton X-100, 1% powdered nonfat dry milk, 0.5% BSA, and 0.02% sodium azide in PBS) to prevent non-specific binding. After another PBS-T wash, embryos were incubated for 18 hours in primary antibody against either BAF155 or BAF170 (BAF155 1:500 dilution, Abcam: cat#ab172638; BAF170 1:500 dilution, Abcam: cat#ab84453). Embryos were subsequently washed three times (30min/wash), followed by incubation in a 1:1000 dilution of a secondary antibody specific to the primary antibody (rabbit IgG conjugated to TRITC, cat#T6778) at 4° C for 12 hours. This staining was followed by three more PBS-T washes and 15min incubation in Hoechst Solution 33324 (2μg/mL; BDbioscience cat: 561908). Embryos were mounted on slides in Vectashield (Vector Laboratories, Burlingame, CA, USA), covered with a glass coverslip and sealed with nail polish. Embryos were examined using a Leica DMi 8 inverted microscope equipped with epifluorescence as well as a Nikon A1R-MP confocal microscope (Leica, Wetzlar, Germany; Nikon, Chiyoda, Japan). Hoechst (blue) was viewed at a wavelength of 405 nm, TRITC (red) was viewed at a wavelength of 561 nm, and GFP (green) was viewed at a wavelength of 488 nm.

5.2 Results

5.2.1 Identification of Nuclear Localization Sequences

Further justification for the likelihood that BAF155 and BAF170 are imported from the cytoplasm to the nucleus via the karyopherin system is the presence of NLS sequences within both subunits' predicted amino acid sequences. Using an NLS sequence predictor, both BAF155 and BAF170 showed strong predicted monopartite and bipartite NLS amino acid sequences (http://nls-mapper.iab.keio.ac.jp/cgi-bin/NLS_Mapper_form.cgi; Table 10).

Table 11: Predicted BAF155 NLS Sequences

BAF155	Position	Sequence	Score
Monopartite	322	NARKRKHSPS	9

Table 12: Predicted BAF170 NLS Sequences

BAF170	Position	Sequence	Score
Monopartite	293	GGNYKKRKRS	9.5
Monopartite	295	NYKKRKRSPS	8
Bipartite	295	NYKKRKRSPSPSPTPEAKKKNAK	10.5
Bipartite	297	KKRKRSPSPSPTPEAKKKNAK	9

The NLS mapping program identifies amino acid nuclear localization sequences specific for karyopherin α/karyopherin β nuclear import pathways. Bipartite nuclear localization sequences are composed of two separate amino acid sequences with a ~10 amino acid space between them. Monopartite nuclear localization sequences do not have an amino acid spacer. The score for each nuclear localization sequence indicates the strength of that specific sequence's activity. Higher scores (8-10) are indicative of nuclear localization sequences completely localized to the nucleus, a middle score (7-8) indicates partial nuclear localization, and a low score (3-5) indicates both nuclear and cytoplasmic localization. The lowest scores (<3) indicate exclusive cytoplasmic localization. There are several sequences in BAF170 which have high scoring,

highly active nuclear localization sequences. The presence of nuclear localization sequences specific to the KPNA/KPNB nuclear import pathway in both BAF155 and BAF170 amino acid sequences, as well as previous data demonstrating the importance of KPNA7 in the porcine preimplantation embryo indicates that KPNA7 is a good candidate for the karyopherin α responsible for nuclear import of BAF155 and/or BAF170.

5.2.2 DN-KPNA7

The DN-KPNA7 experiment included three embryo treatments. The first was the microinjection of the dominant-negative KPNA7 construct tagged with GFP. The second was the microinjection of GFP to show a comparison between DN-KPNA7 GFP fluorescence and distinct GFP fluorescence without being tagged to KPNA. The third group was not injected to show a comparison between injected embryos and unmanipulated embryos and developmental competency of that batch of oocytes. The latter two groups were present as controls for the DN-KPNA7 group.

Figure 10: Localization of BAF155 in porcine 4-cell embryos 48-hours post-treatment. (a) DN-KPNA7 4-cell embryo. (b) GFP 4-cell embryo. (c) Non-Injected 4-cell embryo The first column shows merged images of DNA (Hoechst-blue), BAF155 (TRITC-red) staining, and GFP (green) fluorescence. Then, individual DNA, followed by BAF155 staining, and finally GFP fluorescence. Scale bars, 5 μm.

BAF155 showed expected nuclear localization patterns in the Non-Injected control as well as the GFP-injected control. This indicates that the embryos were viable and that the introduction of GFP did not alter the localization pattern of the BAF155 protein. In the DN-KPNA7 treatment group, the BAF155 embryos maintained their nuclear localization pattern. GFP fluorescence was detected in DN-KPNA7 embryos, indicating translation of the injected mRNA.
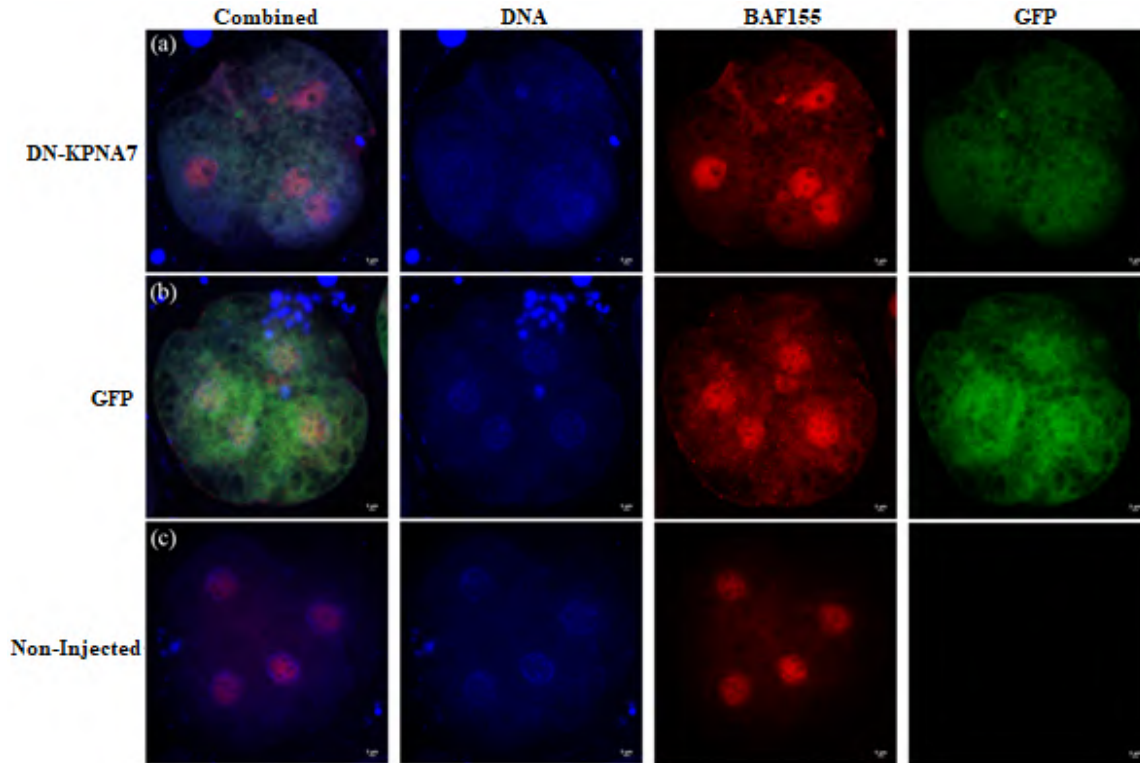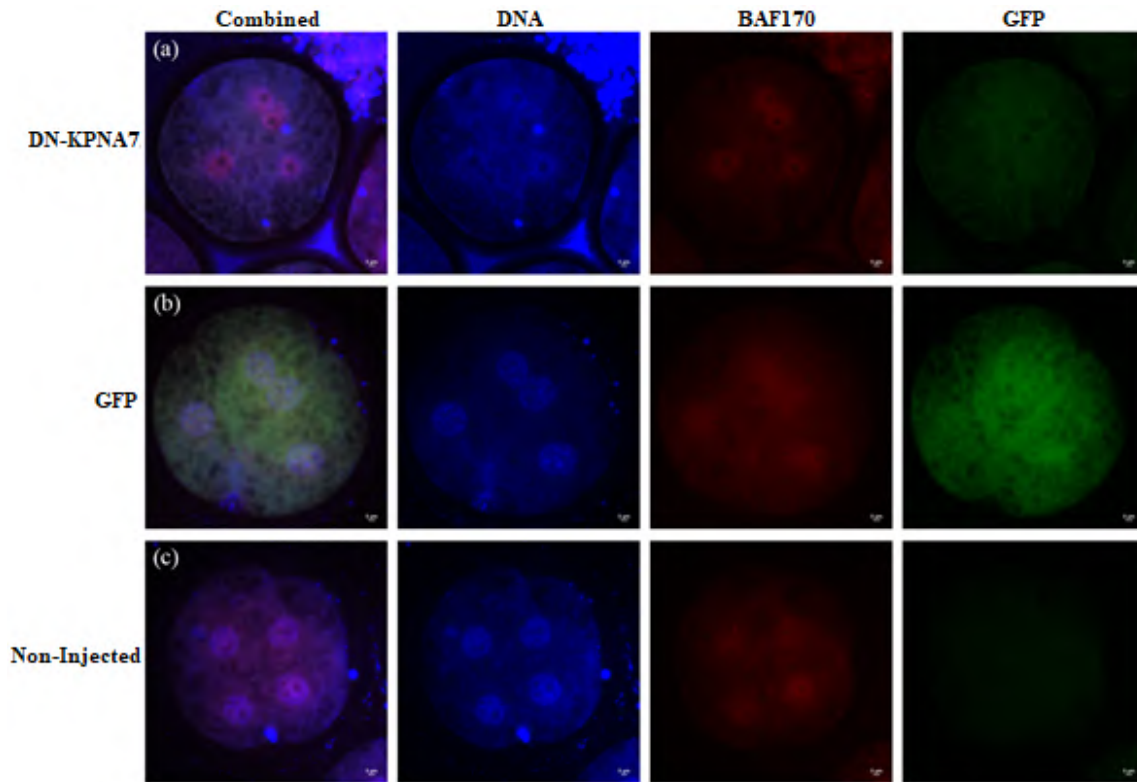
Figure 11: Localization of BAF170 in porcine 4-cell embryos 48-hours post-treatment. (a) DN-KPNA7 4-cell embryo. (b) GFP 4-cell embryo. (c) Non-Injected 4-cell embryo. The first column shows merged images of DNA (Hoechst-blue), BAF170 (TRITC-red) staining, and GFP (green) fluorescence. Then, individual DNA, followed by BAF170 staining, and finally GFP fluorescence. Scale bars, 5 μm.

BAF170 showed expected nuclear localization patterns in the Non-Injected control as well as the GFP-injected control. This indicates that the embryos were viable and that the introduction of GFP did not alter the localization pattern of the BAF170 protein. In the DN-KPNA7 treatment group, the BAF170 embryos maintained their nuclear localization pattern. Again, GFP fluorescence was detected in DN-KPNA7 embryos, indicating translation of the injected mRNA.

Table 13: Four-cell intracellular localization patterns of BAF155 and BAF170 (DN-KPNA7)

Subunit	DN-KPNA7 (4-cell)	GFP (4-cell)	Non-Injected (4-cell)	Average Nuclei # (Day 7)	Average Morph. Blastocyst (Day 7)
BAF155	15/15 (N)	15/15 (N)	24/24 (N)	4.47	7.5% (6/80)
BAF170	22/22 (N)	14/14 (N)	12/12 (N)	5.97	12.5% (8/64)

Three valid replicates were included in this assessment with validity measured by the presence of morphological blastocysts after seven days of in vitro culture of Non-Injected control. N, predominantly nuclear localization. Numbers indicate phenotypic frequency (n/total assessed). Only embryos with 4 visible blastomeres were included in assessment (4-cells). DN-KPNA7 and GFP injected embryos not expressing GFP were excluded from analysis.

Embryos were evaluated on two criteria:

1.) The presence of GFP

2.) The presence of 4 distinct nuclei

For embryos to be included in Table 13, considering the DN-KPNA7 and GFP groups, embryos must be positive for GFP and include 4 distinct nuclei. Considering the Non-Injected group, only 4 distinct nuclei are required for inclusion in Table 13. All embryos which met the necessary requirements maintained the same nuclear localization pattern for BAF155 and BAF170. The presence of morphological blastocysts in the Non-Injected embryos which were cultured to Day 7 was used as a control for embryonic viability. Average morphological blastocyst percentages were calculated as morphological blastocyst per total embryos cultured to Day 7. As a secondary control for embryo viability, average nuclei numbers were calculated as total nuclei per number of Day 7 embryos cultured. All three replicates' nuclei numbers were included in the final

average calculation. Embryos within the treatment groups were not cultured to D7 due to an inability of embryos to develop past D4 following knockdown of KPNA7 (Wang et al. 2012).

5.2.3 RNAi targeting KPNA7

The siRNA experiment targeting KPNA7 included three embryo treatments similar to treatment groups described in Chapter 5. The first was the microinjection of the KPNA7 siRNA.

The second was the microinjection of Scramble RNA to assess any off-targeted effects of the microinjection of a similarly sized RNA molecule not designed to target KPNA7. The third group was not injected to show a comparison between injected embryos and unmanipulated embryos and developmental competency of that batch of oocytes. The latter two groups were present as controls for the KPNA7 siRNA group. Sequences for siRNA targeting KPNA7 and scramble RNA are presented in Table 14 below.

Table 14: KPNA7 siRNA and Scramble Sequences

Targeted	siRNA (antisense)	Scramble-RNA (antisense)
KPNA7	UUGUUAAGGGCGUUAAGCAUUCAUG	UUGCUUGAAUGCGGAAUUUACGAUG

Figure 12 Localization of BAF155 in porcine 4-cell embryos 48-hours post-treatment. (a) KPNA7 siRNA 4-cell embryo. (b) Scramble RNA 4-cell embryo. (c) Non-Injected 4-cell embryo. The first column shows merged images of DNA (Hoechst-blue) and BAF155 (TRITC-red) staining. Then, individual DNA followed by BAF155 staining. Scale bars, 5 μm.

BAF155 showed expected nuclear localization patterns in the Non-Injected control as well as the Scramble RNA control. This indicates that the embryos were viable and that the introduction of the Scramble RNA did not alter the localization pattern of the BAF155 protein. In the KPNA7 siRNA treatment group, the BAF155 embryos maintained their nuclear localization pattern.
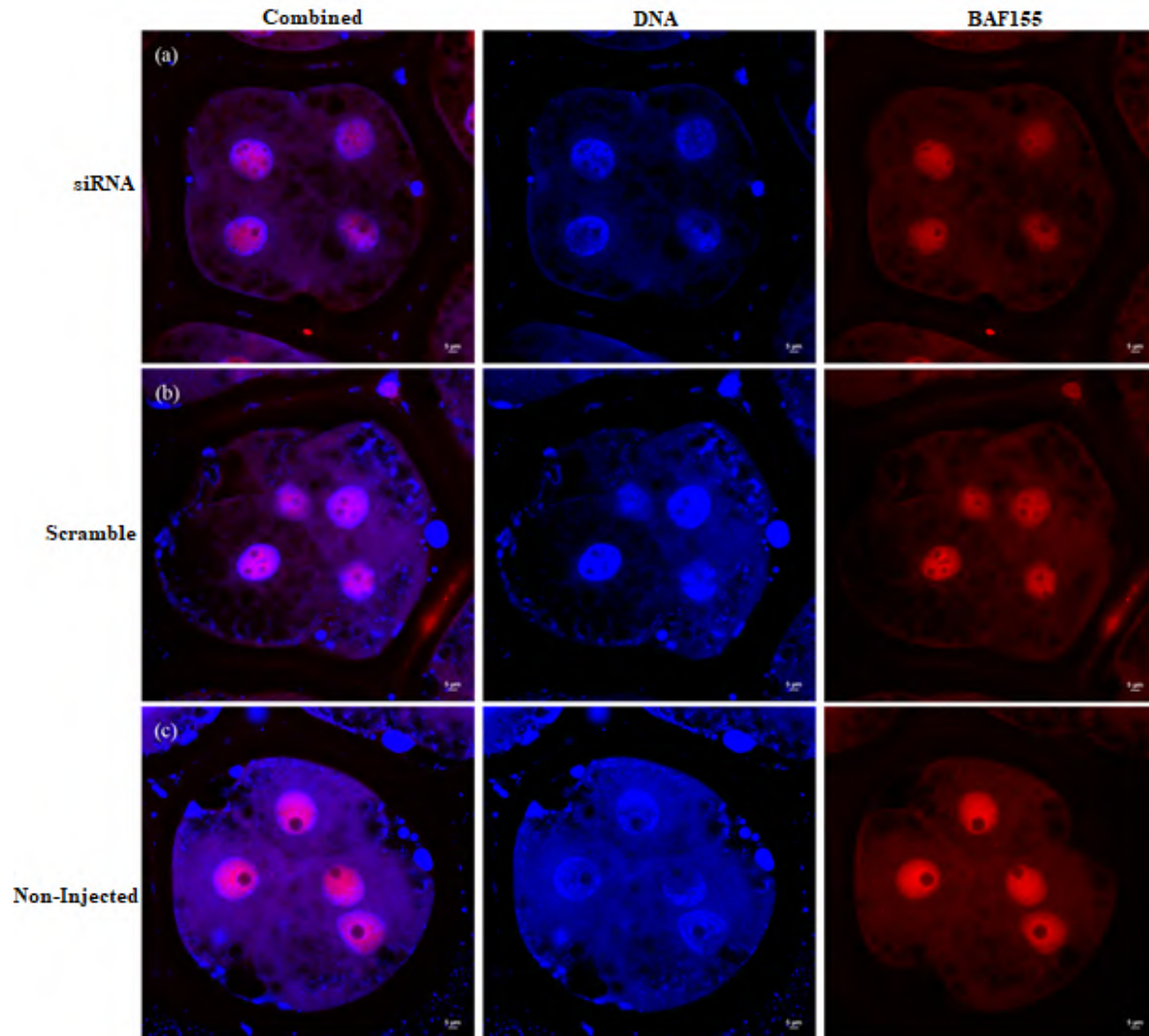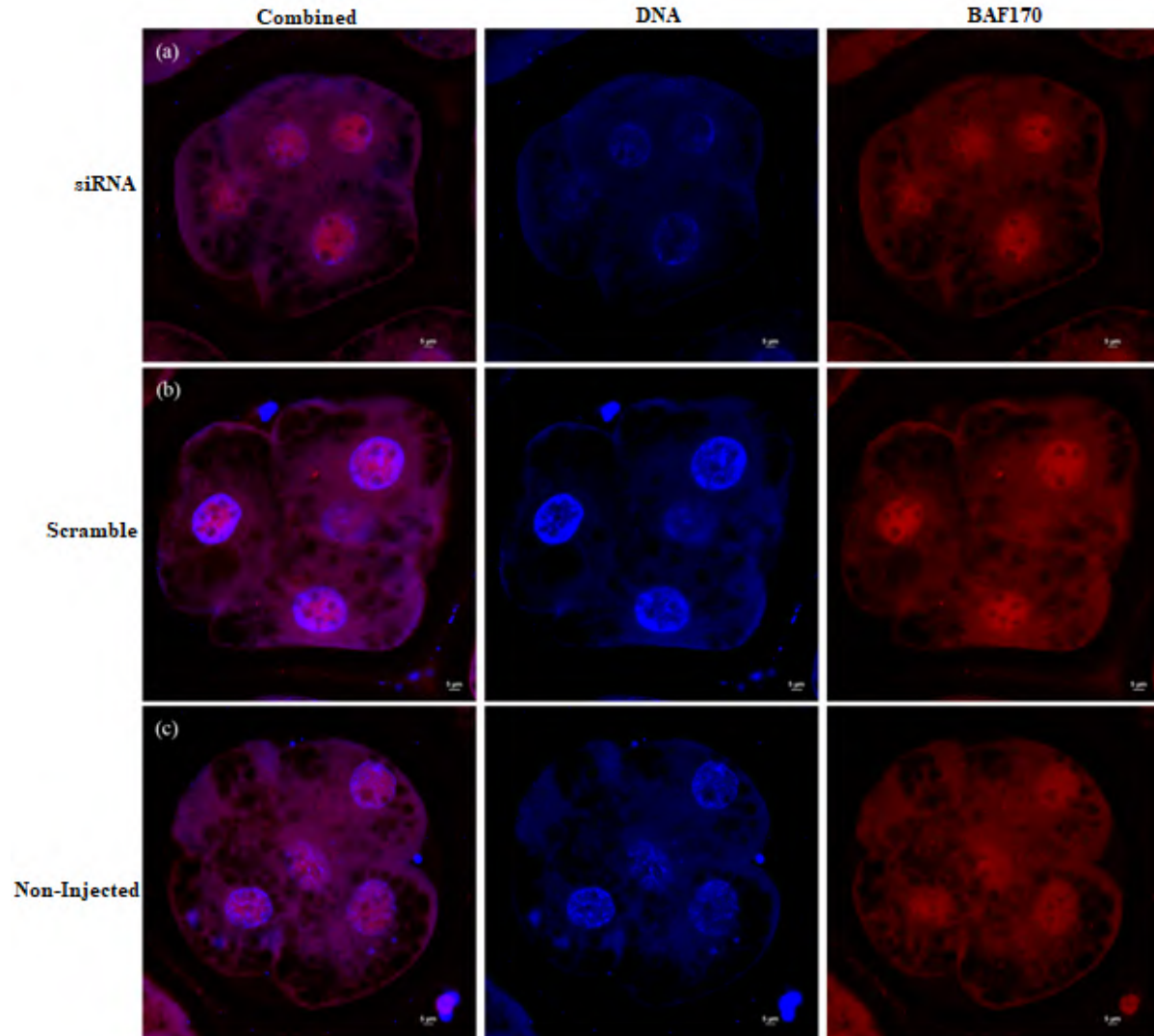
Figure 13: Localization of BAF170 in porcine 4-cell embryos 48-hours post-treatment. (a) KPNA7 siRNA 4-cell embryo. (b) Scramble RNA 4-cell embryo. (c) Non-Injected 4-cell embryo. The first column shows merged images of DNA (Hoechst-blue) and BAF170 (TRITC-red) staining. Then, individual DNA followed by BAF170 staining. Scale bars, 5 μm.

BAF170 showed expected nuclear localization patterns in the Non-Injected control as well as the Scramble RNA control. This indicates that the embryos were viable and that the introduction of the Scramble RNA did not alter the localization pattern of the BAF170 protein. In the KPNA7 siRNA treatment group, the BAF170 embryos maintained their nuclear localization pattern similar to BAF155.

Table 15: Four-cell intracellular localization patterns of BAF155 and BAF170 (KPNA7 siRNA)

Subunit	siRNA (4-cell)	Scramble (4-cell)	Non-Injected (4-cell)	Average Nuclei # (Day 7)	Average Morph. Blastocyst (Day 7)
BAF155	38 (N/N)	26 (N/N)	18 (N/N)	4.55	8.39% (12/143)
BAF170	35 (N/N)	23 (N/N)	20 (N/N)	4.55	8.39% (12/143)

Three valid replicates were included in this assessment with validity measured by the presence of morphological blastocysts after seven days of *in vitro* culture of Non-Injected control. N, predominantly nuclear localization. Numbers indicate phenotypic frequency (n/total assessed). Only embryos with 4 visible blastomeres were included in assessment (4-cells).

Embryos were evaluated on a single criteria:

1.) The presence of 4 distinct nuclei

For embryos to be included in Table 15 embryos must include 4 distinct nuclei. All embryos which met the necessary requirement maintained the same nuclear localization pattern for BAF155 and BAF170. The presence of morphological blastocysts in the Non-Injected embryos, which were cultured to Day 7, was used as a control for embryonic viability. Average morphological blastocyst percentages were calculated as morphological blastocyst per total embryos cultured to Day 7. As a secondary control for embryo viability, average nuclei numbers were calculated as total nuclei per number of Day 7 embryos cultured. All three replicates' nuclei numbers were included in the final average calculation.

All embryos assessed across the three treatment groups and two subunits exhibited nuclear Hoechst staining in addition to nuclear subunit staining.

5.3 Discussion

BAF155 and BAF170 proteins have been shown previously to exhibit nuclear localization in GV oocytes as well as pronuclear, 4-cell, and blastocyst stage porcine embryos (Cabot et al. 2017). Out of the seven karyopherin α proteins, *KPNA7* was most abundant in the porcine GV oocyte with transcript abundance decreasing after the 4-cell stage. KPNA7 protein is nuclear localized in the GV oocyte as well as 2-cell and 4-cell embryos. When siRNA targeting *KPNA7* was injected into embryos, the developmental competency was reduced, and embryos were not able to develop past the 4-cell stage (Wang et al. 2012). This combined data suggests that KPNA7 is important to nuclear import of specific proteins necessary during a critical developmental timeframe.

The localization patterns of BAF155 and BAF170 following overexpression of the *DN-KPNA7* showed no difference between treatment and control groups. The embryos retained their nuclear localization patterns for BAF155 and BAF170. Even though no analysis on fluorescence was performed, fluorescence intensity appeared subjectively of similar intensity. However, during the review of images it was noted that the GFP fluorescence within the *DN-KPNA7* injected embryos remained ubiquitous throughout all three replicates. In the study validating the *DN-KPNA7* construct (Crodian et al. 2019), the GFP fluorescence was cytoplasmic. This was expected, as the *DN-KPNA7* is tagged with *GFP*, and should remain outside the nucleus by design. Because this pattern was not observed, two separately produced batches of mRNA were used to reduce the likelihood that the construct used in the experiment might have been degraded. GFP expression was confirmed, but there could have been a process that left the *GFP* portion of the construct intact while the rest of the *DN-KPNA7* was damaged. When using another batch of construct, the

same fluorescence distribution was observed, indicating that ubiquitous distribution of the construct was likely not caused by faulty construct.

Due to the ubiquitous GFP fluorescence in the *DN-KPNA7* injected group, a new experiment was planned to approach the investigation of nuclear import of BAF155/BAF170 by KPNA7 from a different angle. siRNA targeting *KPNA7* was injected in place of the *DN-KPNA7*, with the experimental protocol otherwise identical. Identical to the results from the *DN-KPNA7* experiment, both BAF155 and BAF170 proteins retained their nuclear localization at the 4-cell stage after ablation of *KPNA7* using the interfering RNA approach.

It is possible that already translated KPNA7 protein is still operating despite the knockdown of *KPNA7*. However, BRD7, which is a ubiquitous protein at the 4-cell stage, shows distinct cytoplasmic and perinuclear localization when microinjected with *DN-KPNA7* or *KPNA7* siRNA following fertilization (Crodian et al. 2019). This indicates that although there is potential for some KPNA7 protein to still be present post-knockdown, there is certainly an effect on the KPNA7 import system using either siRNA or *DN-KPNA7*.

KPNA7 is potentially not the only nuclear importer of BAF155 and BAF170 proteins. Although KPNA7's importance to the early cleavage development of porcine embryos has been shown (Wang et al. 2012), there are six other karyopherin α nuclear import proteins who may play a more significant role than KPNA7 for specific proteins. Future experiments will explore the knockdown of these other six karyopherin αs and the effects on BAF155/BAF170 localization patterns. The presence of strong nuclear localization sequences on both BAF155 and BAF170's amino acid sequences strengthens the hypothesis that they are both imported via a karyopherin α/karyopherin β/cargo trimeric complex.

CHAPTER 6: SUMMARY AND FUTURE DIRECTIONS

The number of couples utilizing assisted reproductive technologies to build their families continues to rise. Unfortunately, the use of *in vitro* embryo production systems has been shown to increase the incidence of epigenetic insult and, subsequently, disorder. Our laboratory explores the ATP-dependent chromatin remodeling SWI/SNF complexes and its dynamic changes throughout porcine preimplantation embryo development. In this thesis, the BAF155 and BAF170 core scaffolding subunits, their effect on embryonic development, and their nuclear import were investigated.

In Chapter 3, BAF155 and BAF170 partial transcripts from porcine tissues were isolated. We hypothesized that BAF155 and BAF170 transcript abundance would change throughout porcine preimplantation embryonic development. mRNA isolated from lysed oocytes and embryos was converted to cDNA. Utilizing this cDNA, we tested transcript abundance of BAF155 and BAF170. However, transcript abundance remained too low to be accurately quantified. This experiment showed that either more highly concentrated cDNA, new qPCR primers, or more sensitive equipment is necessary to accurately quantify the transcript abundance of BAF155 and BAF170 in early porcine embryos.

In Chapter 4 BAF155 and BAF170 siRNA was used to knockdown the transcript of these two subunits post *in vitro* fertilization/activation both individually and in combination. We hypothesized that knockdown of BAF155, BAF170, and/or BAF155/BAF170 would decrease the developmental competency of the porcine embryo. Embryos were divided into three separate treatment groups: (1) siRNA (2) Scramble RNA (3) Non-Injected. All embryos were cultured

until Day 7 and analyzed. Individual nuclei numbers were collected and averaged for each treatment group. Additionally, morphological blastocysts were counted for each group. One-Way ANOVA with Tukey's evaluation of means tests were performed on SAS for both average nuclei numbers and morphological blastocyst percentages. There was no statistical difference for either BAF155, BAF170, or BAF155/BAF170 between the siRNA group and both control groups. This indicated that the differences seen are due to the performance of the microinjection rather than the effect of the siRNA. The results of this study indicate that BAF155 and BAF170 are not critical to the first 7 days of development of the porcine embryo. Alternatively, maternal BAF155 and/or BAF170 proteins may have a long half-life and still be present until the blastocyst stage. To check to see if there is a change in BAF155 and BAF170 protein, immunocytochemistry could be employed in future studies post siRNA knockdown.

Finally, in Chapter 5, we explored the nuclear import of BAF155 and BAF170. We hypothesized that BAF155 and BAF170 would be imported into the nucleus via the KPNA7 pathway. Two separate methods of *KPNA7* knockdown were used: (1) *DN-KPNA7* (2) *KPNA7* siRNA. Both target proteins and DNA were analyzed using immunocytochemistry and Hoechst staining respectively. In both experiments, both BAF155 and BAF170 maintained the nuclear localization pattern seen in the Non-Injected control. This indicates that (1) BAF155 and BAF170 are not imported via the KPNA7 import pathway; (2) BAF155 and BAF170 are imported by another pathway not affected by the KPNA7 knockdown; or (3) maternal BAF155 and BAF170 protein is still present in the nucleus at the 4-cell stage. Other KPNA shuttle proteins (1-6) will be explored as possible nuclear import pathways for BAF155 and BAF170.

The information presented in this thesis provides insight into the developmental requirements and nuclear import of BAF155 and BAF170 SWI/SNF core scaffolding subunits in early porcine

embryos. The hope for this research is to aid in the understanding of chromatin remodeling to increase the viability of *in vitro* derived embryos created with Assisted Reproductive Technologies.

REFERENCES

Aasland R, Stewart AF, Gibson T. "The SANT Domain: a Putative DNA-Binding Domain in the SWI-SNF and ADA Complexes, the Transcriptional Co-Repressor N-CoR and TFIIIB." *Trends in Biomedical Science*, vol. 21, no. 3, 1 March 1996, pp 87-88. Europe PMC, http://europepmc.org/abstract/MED/8882580.

Alpsoy A, and Dykhuizen EC. "Glioma tumor suppressor candidate region gene 1 (GLTSCR1) and its paralog GLTSCR1-like form SWI/SNF chromatin remodeling subcomplexes." *The Journal of Biological Chemistry,* vol. 293, no. 11, 16 March 2018, pp 3892-3903. PubMed, https://www.ncbi.nlm.nih.gov/pubmed/?term=alpsoy+2018+gbaf.

Annunziato A. "DNA Packaging: Nucleosomes and Chromatin." *Nature Education*, vol. 1, no. 1, 2008, pp 26. Scitable, http://origin.www.nature.com/scitable/topicpage/DNA-Packaging-Nucleosomes-and-Chromatin-310.

Bannister AJ, Kouzarides T. "Regulation of chromatin by histone modification." *Cell Research*, vol. 21, no. 3, March 2011, pp 381-395. PMC, https://www.ncbi.nlm.nih.gov/pmc/articles/PMC3193420/.

Bao Y, Shen X. "INO80 subfamily of Chromatin Remodeling Complexes." *Mutation Research*, vol. 618, no. 1-2, 1 May 2007, pp 18-29. PMC, https://www.ncbi.nlm.nih.gov/pmc/articles/PMC2699258/.

Bianchi W, Doe B, Goulding D, Wright GJ. "Juno is the egg Izumo receptor and is essential for mammalian fertilization." *Nature*, vol. 508, 24 April 2014, pp 483-487. Nature, https://www.nature.com/articles/nature13203?error=cookies_not_supported&code=5dbf6b4d-3732-4f9b-b1c5-214f5f311736.

Bos-Mikich A, Bressan FF, Ruggeri RR, Watanabe Y, Meirelles FV. "Parthenogenesis and Human Assisted Reproduction." *Stem Cells International,* 9 November 2015. PMC, https://www.ncbi.nlm.nih.gov/pmc/articles/PMC4655294/.

Boyer LA, Latek RR, Peterson CL. "The SANT Domain: a Unique Histone-Tail-Binding Module?" *Nature Reviews: Molecular Cell Biology*, vol. 5, no. 2, February 2004, pp 158-163. PubMed, https://www.ncbi.nlm.nih.gov/pubmed/15040448.

Bridi M, Abel T. "Histone Modifications in the Nervous System and Neuropsychiatric Disorders." *Epigenetic Regulation in the Nervous System*, December 2013. ResearchGate, https://www.researchgate.net/publication/279946264_Histone_Modifications_in_the_Nervous_System_and_Neuropsychiatric_Disorders.

Burkin HR, Miller DJ. "Zona Pellucida Protein Binding Ability of Porcine Sperm during Epididymal Maturation and the Acrosome Reaction." *Developmental Biology*, vol. 222, no. 1, 1 June 2000, pp 99-109. ScienceDirect, https://www.sciencedirect.com/science/article/pii/S0012160600997070.

Cabot B, Tseng YC, Crodian JS, Cabot R. "Differential Expression of Key Subunits of SWI/SNF Chromatin Remodeling Complexes in Porcine Embryos Derived in Vitro or in Vivo." *Molecular Reproduction and Development*, vol. 84, no. 12, December 2017, pp 1238-1249. PubMed, https://www.ncbi.nlm.nih.gov/pubmed/29024220.

Cairns BR, Lorch Y, Li Y, Zhang M, Lacomis L, Erdjument-Bromage H, Tempst P, Du J, Laurent B, Kornberg RD. "RSC, an Essential, Abundant Chromatin-Remodeling Complex." *Cell*, vol. 87, no. 7, 27 December 1996, pp 1249-1260. PubMed, https://www.ncbi.nlm.nih.gov/pubmed/8980231.

Chen J, Archer TK. "Regulating SWI/SNF subunit levels via protein-protein interactions and proteasomal degradation: BAF155 and BAF170 limit expression of BAF57." *Molecular and Cellular Biology*, vol. 25, no. 20, October 2005, pp 9016-9027. PMC, https://www.ncbi.nlm.nih.gov/pmc/articles/PMC1265786/.

Chook YM, Blobel G. "Karyopherins and Nuclear Import." *Current Opinion in Structural Biology*, vol. 11, no. 6, December 2001, pp 703-715. PubMed, https://www.ncbi.nlm.nih.gov/pubmed/11751052.

Clapier CR, Cairns BR. "The Biology of Chromatin Remodeling Complexes." *Annual Review of Biochemistry*, vol. 78, 2009, pp 273-304. PubMed, https://www.ncbi.nlm.nih.gov/pubmed/19355820.

Clements A, Poux AN, Lo WS, Pillus L, Berger SL, Marmorstein R. "Structural Basis for Histone and Phosphohistone Binding by the GCN5 Histone Acetyltransferase." *Molecular Cell*, vol. 12, no. 2, August 2003, pp 461-473. PubMed, https://www.ncbi.nlm.nih.gov/pubmed/14536085.

Crodian JS, Weldon BM, Tseng YC, Cabot B, Cabot R. "Nuclear trafficking dynamics of BRD7, a SWI/SNF chromatin remodeling complex subunit, in porcine oocytes and cleavage stage embryos." *Reproduction, Fertility, and Development,* 13 May 2019. PubMed, https://www.ncbi.nlm.nih.gov/pubmed/31079594.

de la Serna IL, Ohkawa Y, Imbalzano AN. "Chromatin Remodelling in Mammalian Differentiation: Lessons from ATP-Dependent Remodellers." *Nature Reviews: Genetics*, vol. 7, no. 6, June 2006, pp 461-473. PubMed, https://www.ncbi.nlm.nih.gov/pubmed/16708073.

Fan HY, Trotter KW, Archer TK, Kingston RE. "Swapping Function of Two Chromatin Remodeling Complexes." *Molecular Cell*, vol. 17, no. 6, 18 March 2005, pp 805-815. PubMed, https://www.ncbi.nlm.nih.gov/pubmed/15780937.

Flaus A, Owen-Hughes T. "Mechanisms for ATP-dependent chromatin remodelling: the means to the end." *The FEBS Journal*, vol. 278, no. 19, October 2011, pp 3579-3595. PubMed, https://www.ncbi.nlm.nih.gov/pubmed/21810178.

Fuhua X, Flowers S, Moran E. "Essential role of ARID2 protein-containing SWI/SNF complex in tissue-specific gene expression." *Journal of Biological Chemistry*, vol. 287, no. 7, 10 February 2012, pp 5033-5041. PMC, https://www.ncbi.nlm.nih.gov/pmc/articles/PMC3281626/.

Fujisawa T, Filippakopoulos P. "Functions of Bromodomain-Containing Proteins and Their Roles in Homeostasis and Cancer." *Nature Reviews: Molecular Cell Biology*, vol. 18, no. 4, April 2017, pp 246-262. PubMed, https://www.ncbi.nlm.nih.gov/pubmed/28053347.

Gao X, Tate P, Hu P, Tijan R, Skarnes WC, Wang Z. "ES cell pluripotency and germ-layer formation require the SWI/SNF chromatin remodeling component BAF250a." *Proceedings of the National Academy of Sciences of the United States of America*, vol. 105, no. 18, 6 May 2008, pp 6656-6661. PubMed, https://www.ncbi.nlm.nih.gov/pubmed/18448678.

Gruene T, Brzeski J, Eberharter A, Clapier CR, Corona DF, Becker PB, Mueller CW. "Crystal Structure and Functional Analysis of a Nucleosome Recognition Module of the Remodeling Factor ISWI." *Molecular Cell*, vol. 12, no. 2, August 2003, pp 449-460. PubMed, https://www.ncbi.nlm.nih.gov/pubmed/14536084.

Grunstein M. "Histone Acetylation in Chromatin Structure and Transcription." *Nature*, vol. 389, no. 6649, 24 September 1997, pp 349-352. PubMed, https://www.ncbi.nlm.nih.gov/pubmed/9311776.

Guidi CJ, Sands AT, Zambrowicz BP, Turner TK, Demers DA, Webster W, Smith TW, Imbalzano AN, Jones SN. "Disruption of Ini1 Leads to Peri-Implantation Lethality and Tumorigenesis in Mice." *Molecular and Cellular Biology*, vol. 21, no. 10, May 2001, pp 3598-3603. PubMed Central, https://www.ncbi.nlm.nih.gov/pmc/articles/PMC100281/.

Harmacek L, Watkins-Chow DE, Chen J, Jones KL, Pavan WJ, Salbaum JM, Niswander L. "A Unique Missense Allele of BAF155, a Core BAF Chromatin Remodeling Complex Protein, Causes Neural Tube Closure Defects in Mice." *Developmental Neurobiology,* vol. 74, no. 5, May 2014, pp 483-497. PubMed Central, https://www.ncbi.nlm.nih.gov/pmc/articles/PMC4670623/.

He J, Xuan T, Xin T, An H, Wang J, Zhao G, Li M. "Evidence for chromatin-remodeling complex PBAP-controlled maintenance of the Drosophila ovarian germline stem cells." *PloS* One, vol. 9, no. 7, 28 July 2014. PubMed, https://www.ncbi.nlm.nih.gov/pubmed/25068272.

Ho L, Crabtree GR. "Chromatin remodelling during development." *Nature*, vol. 463, no. 7280, 28 January 2010, pp 474-484. PubMed, https://www.ncbi.nlm.nih.gov/pubmed/20110991.

Ho L, Ronan JL, Wu J, Staahl BT, Chen L, Kuo A, Lessard J, Nesvizhskii AI, Ranish J, Crabtree JR. "An embryonic stem cell chromatin remodeling complex, esBAF, is essential for embryonic stem cell self-renewal and pluripotency." *Proceedings of the National Academy of Sciences of the United States of America*, vol. 106, no. 13, 31 March 2009, pp 5181-5186. PubMed, https://www.ncbi.nlm.nih.gov/pubmed/19279220.

Hodges C, Kirkland JG, Crabtree GR. "The Many Roles of BAF (mSWI/SNF) and PBAF Complexes in Cancer." *Cold Spring Harbor Perspectives in Medicine*, vol. 6, no. 8, August 2016. PMC, https://www.ncbi.nlm.nih.gov/pmc/articles/PMC4968166/.

Hou L, Ma F, Yang J, Riaz H, Wang Y, Wu W, Xia X, Ma Z, Zhou Y, Zhang L, Ying W, Xu D, Zuo B, Ren Z, Xiong Y. "Effects of histone deacetylase inhibitor oxamflatin on in vitro porcine somatic cell nuclear transfer embryos." *Cellular Reprogramming*, vol. 16, no. 4, August 2014, pp 253-265. PubMed, https://www.ncbi.nlm.nih.gov/pubmed/24960409.

Ikawa M, Inoue N, Benham AM, Okabe M. "Fertilization: a sperm's journey to and interaction with the oocyte." *The Journal of Clinical Investigation*, vol. 120, no. 4, 1 April 210, pp 984-994. PMC, https://www.ncbi.nlm.nih.gov/pmc/articles/PMC2846064/.

Jeppesen P, Turner BM. "The Inactive X Chromosome in Female Mammals Is Distinguished by a Lack of Histone H4 Acetylation, a Cytogenetic Marker for Gene Expression." *Cell*, vol. 74, no. 2, 30 July 1993, pp 281-289. PubMed, https://www.ncbi.nlm.nih.gov/pubmed/8343956.

Jiang Z, Tang Y, Zhao X, Zhang M, Donovan DM, Tian XC. "Knockdown of Brm and Baf170, Components of Chromatin Remodeling Complex, Facilitates Reprogramming of Somatic Cells." *Stem Cells and Development*, vol. 24, no. 19, 1 October 2015, pp 2328-2336. PubMed, https://www.ncbi.nlm.nih.gov/pubmed/26121422.

Jukam D, Shariati SAM, Skotheim JM. "Zygotic Genome Activation in Vertebrates." *Developmental Cell*, vol. 42, no. 4, 21 August 2017, pp 316-332. ScienceDirect, https://www.sciencedirect.com/science/article/pii/S1534580717306020.

Jung I, Sohn DH, Choi J, Kim JM, Jeon S, Seol JH, Seong RH. "SRG3/mBAF155 stabilizes the SWI/SNF-like BAF complex by blocking CHFR mediated ubiquitination and degradation of its major components." *Biochemical and Biophysical research communications,* vol. 418, no. 3, 17 February 2012, pp 512-517. PubMed, https://www.ncbi.nlm.nih.gov/pubmed/22285184.

Kadoch C, Crabtree GR. "Mammalian SWI/SNF chromatin remodeling complexes and cancer: Mechanistic insights gained from human genomics." *Science Advances*, vol. 1, no. 5, 12 June 2015. Science Advances, http://advances.sciencemag.org/content/1/5/e1500447.

Kanka J, Kepkova K, Nemkova L. "Gene Expression during Minor Genome Activation in Preimplantation Bovine Development." *Theriogenology*, vol. 72, no. 4, 1 September 2009, pp 572-583. PubMed, https://www.ncbi.nlm.nih.gov/pubmed/19501393.

Kelley JB, Talley AM, Spencer A, Gioeli D, Paschal BM. "Karyopherin alpha7 (KPNA7), a divergent member of the importin alpha family of nuclear import receptors." *BMC Cell Biology*, vol. 11, no. 63, 11 August 2010. PubMed, https://www.ncbi.nlm.nih.gov/pubmed/20701745.

Kharche SD, Birade HS. "Parthenogenesis and Activation of Mammalian Oocytes for in Vitro Embryo Production: A Review." *ABB*, vol. 4, no. 2, February 2013. Scientific Research, https://www.scirp.org/journal/PaperInformation.aspx?PaperID=28406.

Khavari PA, Peterson CL, Tamkun JW, Mendel DB, Crabtree GR. "BRG1 Contains a Conserved Domain of the SWI2/SNF2 Family Necessary for Normal Mitotic Growth and Transcription." *Nature*, vol. 366, no. 6451, 11 November 1993, pp 170-174. PubMed, https://www.ncbi.nlm.nih.gov/pubmed/8232556.

Kidder BL, Palmer S, Knott JG. "SWI/SNF-Brg1 Regulates Self-Renewal and Occupies Core Pluripotency-Related Genes in Embryonic Stem Cells." *Stem Cells*, vol. 27, no. 2, February 2009, pp 317-328. PubMed, https://www.ncbi.nlm.nih.gov/pubmed/19056910.

Laity JH, Lee BM, Wright PE. "Zinc Finger Proteins: New Insights into Structural and Functional Diversity." *Current Opinion in Structural Biology*, vol. 11, no. 1, February 2001, pp 39-46. PubMed, https://www.ncbi.nlm.nih.gov/pubmed/11179890.

Lee K, Hamm J, Whitworth K, Spate L, Park KW, Murphy CN, Prather RS. "Dynamics of TET Family Expression in Porcine Preimplantation Embryos Is Related to Zygotic Genome Activation and Required for the Maintenance of NANOG." *Developmental Biology*, vol. 386, no. 1, 1 February 2014, pp 86-95. Science Direct, https://www.sciencedirect.com/science/article/pii/S0012160613006416.

Lee MT, Bonneau AR, Giraldez AJ. "Zygotic genome activation during the maternal-to-zygotic transition." *Annual Review of Cell and Developmental Biology*, vol. 30, 2012, pp 581-613. PMC, https://www.ncbi.nlm.nih.gov/pmc/articles/PMC4303375/.

Lessard JA, Crabtree GR. "Chromatin regulatory mechanisms in pluripotency." *Annual Review of Cell and Developmental Biology*, vol.26, 2010, pp 503-532. PubMed, https://www.ncbi.nlm.nih.gov/pubmed/20624054.

Lewin, Benjamin. *Genes VII*. Oxford, Oxford University Press, 9 December 1999.

Li J, Mahajan A, Tsai MD. "Ankyrin Repeat: a Unique Motif Mediating Protein-Protein Interactions." *Biochemistry*, vol. 45, no. 51, 26 December 2006, pp 15168-15178. PubMed, https://www.ncbi.nlm.nih.gov/pubmed/17176038.

Lomeli H, Castillo-Robles J. "The Developmental and Pathogenic Roles of BAF57, a Special Subunit of the BAF Chromatin-Remodeling Complex." *FEBS Letters*, vol. 590, no. 11, June 2016, pp 1555-1569. PubMed, https://www.ncbi.nlm.nih.gov/pubmed/27149204.

Lu YH, Wang N, Jin F. "Long-term follow-up of children conceived through assisted reproductive technology." *Journal of Zhejiang University Science B*, vol. 14, no. 5, May 2013, pp 359-371. PMC, https://www.ncbi.nlm.nih.gov/pmc/articles/PMC3650450/.

Machaty Z, Miller AR, Zhang L. "Egg Activation at Fertilization." *Advances in Experimental Medicine and Biology*, vol. 953, 2017, pp 1-47. PubMed, https://www.ncbi.nlm.nih.gov/pubmed/27975269.

Magnani L, Cabot RA. "Developmental Arrest Induced in Cleavage Stage Porcine Embryos Following Microinjection of MRNA Encoding Brahma (Smarca 2), a Chromatin Remodeling Protein." *Molecular Reproduction and Development*, vol. 74, no. 10, October 2007, pp 1262-1267. PubMed, https://www.ncbi.nlm.nih.gov/pubmed/17342730.

Magnani L, Cabot RA. "Manipulation of SMARCA2 and SMARCA4 Transcript Levels in Porcine Embryos Differentially Alters Development and Expression of SMARCA1, SOX2, NANOG, and EIF1." *Reproduction*, vol. 137, no. 1, January 2009, pp 23-33. PubMed, https://www.ncbi.nlm.nih.gov/pubmed/18845624.

Marquez-Vilendrer SB, Rai SK, Gramling SJB, Lu L, Reisman DN. "Loss of the SWI/SNF ATPase subunits BRM and BRG1 drives lung cancer development." *Oncoscience*, vol. 3, no. 11-12, 2016, pp 322-336. PMC, https://www.ncbi.nlm.nih.gov/pmc/articles/PMC5235921/.

Mashtalir N, D'Avino AR, Michel BC, Luo J, Pan J, Otto JE, Zullow HJ, McKenzie ZM, Kubiak RL, St. Pierre R, Valencia AM, Poynter SJ, Cassel SH, Ranish JA, Kadoch C. "Modular Organization and Assembly of SWI/SNF Family Chromatin Remodeling Complexes." *Cell,* vol. 135, no. 5, 15 November 2018, pp 1272-1288. ScienceDirect, https://www.sciencedirect.com/science/article/pii/S0092867418312443?via%3Dihub.

Metzger E, Yin N, Wissmann M, Kunowska N, Fischer K, Friedrichs N, Patnaik D, Higgins JM, Potier N, Scheidtmann KH, Buettner R, Schuele R. "Phosphorylation of Histone H3 at Threonine 11 Establishes a Novel Chromatin Mark for Transcriptional Regulation." *Nature Cell Biology*, vol. 10, no. 1, January 2008, pp 53-60. PubMed, https://www.ncbi.nlm.nih.gov/pubmed/18066052.

Mirabella AC, Foster BM, Bartke T. "Chromatin deregulation in disease." *Chromosoma*, vol. 125, no. 1, March 2016, pp 75-93. PubMed, https://www.ncbi.nlm.nih.gov/pubmed/26188466.

Narayanan R, Pirouz M, Kerimoglu C, Pham L, Wagener RJ, Kiszka KA, Rosenbusch J, Seong RH, Kessel M, Fischer A, Stoykova A, Staiger JF, Tuoc T. "Loss of BAF (mSWI/SNF) Complexes Causes Global Transcriptional and Chromatin State Changes in Forebrain Development." *Cell Reports*, vol. 13, no. 9, 1 December 2015, pp 1842-1854. PubMed, https://www.ncbi.nlm.nih.gov/pubmed/26655900.

Ng SS, Yue WW, Oppermann U, Klose RJ. "Dynamic Protein Methylation in Chromatin Biology." *Cellular and Molecular Life Sciences*, vol. 66, no. 3, February 2009, pp 407-422. PubMed, https://www.ncbi.nlm.nih.gov/pubmed/18923809.

Oh IH, Reddy EP. "The Myb Gene Family in Cell Growth, Differentiation and Apoptosis." *Oncogene*, vol. 18, no. 19, 13 May 1999, pp 3017-3033. PubMed, https://www.ncbi.nlm.nih.gov/pubmed/10378697.

Oike T, Ogiwara H, Amornwichet N, Nakano T, Kohno T. "Chromatin-regulating proteins as targets for cancer therapy." *Journal of Radiation Research*, vol. 55, no. 4, February 2014. ResearchGate, https://www.researchgate.net/publication/260169111_Chromatin-regulating_proteins_as_targets_for_cancer_therapy.

Phelan ML, Sif S, Narliker GJ, Kingston RE. "Reconstitution of a Core Chromatin Remodeling Complex from SWI/SNF Subunits." *Molecular Cell*, vol. 3, no. 2, 3 February 1999, pp 247-253. PubMed, https://www.ncbi.nlm.nih.gov/pubmed/10078207.

Razin A, Cedar H. "DNA methylation and gene expression." *Microbiological Reviews*, vol. 55, no. 3, September 1991, pp 451-458. PubMed, https://www.ncbi.nlm.nih.gov/pubmed/1943996.

Rizos D, Clemente M, Bermejo-Alvarez P, de La Fuente J, Lonergan P, Gutierrez-Adan A. "Consequences of in Vitro Culture Conditions on Embryo Development and Quality." *Reproduction in Domestic Animals*, vol. 43, October 2008, pp 44-50. PubMed, https://www.ncbi.nlm.nih.gov/pubmed/18803756.

Rossetto D, Avvakumov N, Cote J. "Histone phosphorylation: a chromatin modification involved in diverse nuclear events." *Epigenetics*, vol. 7, no. 10, October 2012, pp 1098-1108. PubMed, https://www.ncbi.nlm.nih.gov/pubmed/22948226.

Sanchez R, Zhou MM. "The PHD finger: a versatile epigenome reader." *Trends in Biochemical Sciences*, vol. 36, no. 7, July 2011, pp 364-372. PubMed, https://www.ncbi.nlm.nih.gov/pubmed/21514168.

Santen GW, Kriek M, van Attikum H. "SWI/SNF complex in disorder: SWItching from malignancies to intellectual disability." *Epigenetics*, vol. 7, no. 11, November 2012, pp 1219-1224. PubMed, https://www.ncbi.nlm.nih.gov/pubmed/23010866.

Schlensted G. "Protein Import into the Nucleus." *FEBS Letters*, vol. 389, no. 1, 24 June 1996, pp 75-79. ScienceDirect, https://www.sciencedirect.com/science/article/pii/0014579396005832.

Segre C, Chiocca S. "Regulating the regulators: the post-translational code of class I HDAC1 and HDAC2." *Journal of Biomedicine and Biotechnology*, no. 16, 2011. ResearchGate, https://www.researchgate.net/publication/49720478_Regulating_the_regulators_The_post-translational_code_of_class_I_HDAC1_and_HDAC2.

Shen X, Ranallo R, Choi E, Wu C. "Involvement of Actin-Related Proteins in ATP-Dependent Chromatin Remodeling." *Molecular Cell*, vol. 12, no. 1, July 2003, pp 147-155. PubMed, https://www.ncbi.nlm.nih.gov/pubmed/12887900.

Singh AP, Foley JF, Rubino M, Boyle MC, Tandon A, Shah R, Archer TK. "Brg1 Enables Rapid Growth of the Early Embryo by Suppressing Genes That Regulate Apoptosis and Cell Growth Arrest." *Molecular and Cellular Biology*, vol. 36, no. 15, 14 July 2016, pp 1990-2010. PubMed, https://www.ncbi.nlm.nih.gov/pubmed/27185875.

Singhal N, Esch D, Stehling M, Schoeler HR. "BRG1 Is Required to Maintain Pluripotency of Murine Embryonic Stem Cells." *BioResearch Open Access*, vol. 3, no. 1, 1 February 2014, pp 1-8. PMC, https://www.ncbi.nlm.nih.gov/pmc/articles/PMC3929005/.

Snider AC, Leong D, Wang QT, Wysocka J, Tao MW, Scott MP. "The chromatin remodeling factor Chd1l is required in the preimplantation embryo." *Biology Open*, vol. 2, no. 2, 15 February 2013, pp 121-131. PubMed, https://www.ncbi.nlm.nih.gov/pubmed/23429299.

Sohn DH, Lee KY, Lee C, Oh J, Chung H, Jeon SH, Seong RH. "SRG3 Interacts Directly with the Major Components of the SWI/SNF Chromatin Remodeling Complex and Protects Them from Proteasomal Degradation." *The Journal of Biological Chemistry,* vol. 282, 6 April 2007, pp 10614-10624. Journal of Biological Chemistry. http://www.jbc.org/content/282/14/10614.long.

Sullivan-Pyke CS, Senapati S, Mainigi MA, Barnhart KT. "In Vitro fertilization and adverse obstetric and perinatal outcomes." *Seminars in Perinatology*, vol. 41, no. 6, October 2017, pp 345-353. PubMed, https://www.ncbi.nlm.nih.gov/pubmed/28818301.

Svoboda P. "Mammalian Zygotic Genome Activation." *Seminars in Cell and Developmental Biology*, vol. 84, December 2018, pp 118-126. ScienceDirect, https://www.sciencedirect.com/science/article/pii/S1084952117300563.

Tang L, Nogales E, Ciferri C. "Structure and function of SWI/SNF chromatin remodeling complexes and mechanistic implications for transcription." *Progress in Biophysics and Molecular Biology*, vol. 102, no. 2-3, June-July 2010, pp 122-128. PubMed, https://www.ncbi.nlm.nih.gov/pubmed/20493208.

Tejomurtula J, Lee KB, Tripurani SK, Smith GW, Yao J. "Role of Importin alpha8, a New Member of the Importin Alpha Family of Nuclear Transport Proteins, in Early Embryonic Development in Cattle." *Biology of Reproduction*, vol. 81, no. 2, August 2009, pp 333-342. PubMed, https://www.ncbi.nlm.nih.gov/pubmed/19420384.

Tienthai P, Johannisson A, Rodriguez-Martinez H. "Sperm Capacitation in the Porcine Oviduct." *Animal Reproduction Science*, vol. 80, no. 1-2, January 2004, pp 131-146. PubMed, https://www.ncbi.nlm.nih.gov/pubmed/15036522.

Trotter KW, Archer TK. "The BRG1 transcriptional coregulator." *Nuclear Receptor Signaling*, vol. 6, 2008. PMC, https://www.ncbi.nlm.nih.gov/pmc/articles/PMC2254329/.

Tseng YC, Cabot B, Cabot RA. "ARID1A, a component of SWI/SNF chromatin remodeling complexes, is required for porcine embryo development." *Molecular Reproduction and Development*, vol. 84, no. 12, December 2017, pp 1250-1256. PubMed Central. https://www.ncbi.nlm.nih.gov/pmc/articles/PMC5760285/.

Tuoc TC, Boretius S, Sansom SN, Pitulescu ME, Frahm J, Livesey FJ, Stoykova A. "Chromatin Regulation by BAF170 Controls Cerebral Cortical Size and Thickness." *Developmental Cell*, vol. 258, no. 3, 13 May 2013, pp 256-269. PubMed, https://www.ncbi.nlm.nih.gov/pubmed/23643363.

Tuoc TC, Narayanan R, Stoykova A. "BAF chromatin remodeling complex: cortical size regulation and beyond." *Cell Cycle*, vol. 12, no. 18, 15 September 2013, pp 2953-2959. PubMed, https://www.ncbi.nlm.nih.gov/pubmed/23974113.

Turner BM, Birley AJ, Lavender J. "Histone H4 Isoforms Acetylated at Specific Lysine Residues Define Individual Chromosomes and Chromatin Domains in Drosophila Polytene Nuclei." *Cell*, vol. 69, no. 2, 17 April 1992, pp 375-384. PubMed, https://www.ncbi.nlm.nih.gov/pubmed/1568251.

Vignali M, Hassan AH, Neely KE, Workman JL. "ATP-dependent chromatin-remodeling complexes." *Molecular and Cellular Biology*, vol. 20, no. 6, 2000, pp 1899-1910. American Society for Microbiology, https://mcb.asm.org/content/20/6/1899.

Wang X, Lee RS, Alver BH, Haswell JR, Wang S, Mieczkowski J, Drier Y, Gillespie SM, Archer TC, Wu JN, Tzvetkov EP, Troisi EC, Pomeroy SL, Biegel JA, Tolstorukov MY, Bernstein BE, Park PJ, Roberts CW. "SMARCB1-mediated SWI/SNF complex function is essential for enhancer regulation." *Nature Genetics*, vol. 49, no. 2, February 2017, pp 289-295. PubMed, https://www.ncbi.nlm.nih.gov/pubmed/27941797.

Wang X, Park KE, Koser S, Liu S, Magnani L, Cabot RA. "KPNA7, An Oocyte- and Embryo-Specific Karyopherin α Subtype, Is Required for Porcine Embryo Development." *Reproduction, Fertility, and Development*, vol. 24, no. 2, 2012, pp 382-391. PubMed, https://www.ncbi.nlm.nih.gov/pubmed/22281085.

Wente SR, Rout MP. "The nuclear pore complex and nuclear transport." *Cold Spring Harbor Perspectives in Biology*, vol. 2, no. 10, 2010. PMC, https://www.ncbi.nlm.nih.gov/pmc/articles/PMC2944363/.

Whitworth KM, Agca C, Kim JG, Patel RV, Springer GK, Bivens NJ, Forrester LJ, Mathialagan N, Green JA, Prather RS. 2005. Transcriptional profiling of pig embryogenesis by using a 15-K member unigene set specific for pig reproductive tissues and embryos. Biol Reprod 72:1437–1451.

Xu, F., Flowers, S., & Moran, E. "Essential role of ARID2 protein☐containing SWI/SNF complex in tissue☐specific gene expression." *The Journal of Biological Chemistry*, vol. 287, no. 7, pp 5033–5041, 2012. PMC, https://doi.org/10.1074/jbc.M111.279968

Yan Z, Wang Z, Sharova L, Sharov AA, Ling C, Piao Y, Aiba K, Matoba R, Wang W, Ko MS. "BAF250B-associated SWI/SNF chromatin-remodeling complex is required to maintain undifferentiated mouse embryonic stem cells." *Stem Cells*, vol. 26, no. 5, May 2008, pp 1155-1165. PubMed, https://www.ncbi.nlm.nih.gov/pubmed/18323406.

Yildirim O, Li Rm Hung JH, Chen PB, Dong X, Ee LS, Weng Z, Rando OJ, Fazzio TG. "Mbd3/NURD complex regulates expression of 5-hydroxymethylcytosine marked genes in embryonic stem cells." *Cell*, vol. 147, no. 7, 23 December 2011, pp 1498-1510. PubMed, https://www.ncbi.nlm.nih.gov/pubmed/22196727.

Zhang X, Li B, Li W, Ma L Zheng D, Li L, Yang W, Chu M, Chen W, Mailman RB, Zhu J, Fan G, Archer TK, Wang Y. "Transcriptional repression by the BRG1-SWI/SNF complex affects the pluripotency of human embryonic stem cells." *Stem Cell Report*, vol. 3, no. 3, 9 September 2014, pp 460-474. PubMed, https://www.ncbi.nlm.nih.gov/pubmed/25241744.

Zheng P, Patel B, McMenamin M, Paprocki AM, Schramm RD, Nagl NG Jr, Wilsker D, Wang X, Moran E, Latham KE. "Expression of genes encoding chromatin regulatory factors in developing rhesus monkey oocytes and preimplantation stage embryos: possible roles in genome activation." *Biology of Reproduction*, vol. 70, no. 5, 14 January 2004, pp 1419-27. PubMed. https://www.ncbi.nlm.nih.gov/pubmed/14724134/.

Zhu J, King T, Dobrinsky J, Harkness L, Ferrier T, Bosma W, Schreier LL, Guthrie HD, DeSousa P, Wilmut I. "In Vitro and In Vivo Developmental Competence of Ovulated and In Vitro Matured Porcine Oocytes Activated by Electrical Activation." *Cloning and Stem Cells,* vol. 5, no. 4, 2003. Semantic Scholar. https://pdfs.semanticscholar.org/cc93/a293d1c4eb9ba7355984c12076bb331663b2.pdf.